

LATTICE QCD AT THE INTENSITY FRONTIER

Thomas Blum, Michael Buchoff, Norman Christ, Andreas Kronfeld,
Paul Mackenzie, Stephen Sharpe, Robert Sugar and Ruth Van de Water

(USQCD Collaboration)

(Dated: October 22, 2013)

CONTENTS

I. EXECUTIVE SUMMARY

II. INTRODUCTION

III. CURRENT STATUS OF LATTICE QCD

III A. Validation of lattice QCD methodology

III B. Quark flavor physics

III C. Summary

IV. FUTURE LATTICE CALCULATIONS

IV A. Quark flavor physics

IV B. Charged lepton physics: $g-2$ and $\text{Mu}2e$

IV C. Neutrino physics, underground physics, and related processes

IV D. Precision Higgs physics: improvements to quark masses and α_s

V. RESOURCES FOR STUDIES AT THE INTENSITY FRONTIER

V A. DWF resource requirements

V B. HISQ resource requirements

VI. SUMMARY

Appendix: Future prospects

A. Standard lattice matrix elements

B. More challenging Lattice QCD calculations

I. EXECUTIVE SUMMARY

This white paper describes the opportunities for lattice QCD (LQCD) to play a key role in supporting the future experimental high-energy physics program in tests of the Standard Model and searches for new physics. Lattice calculations are most broadly relevant for experiments at the intensity frontier, but they will also play key roles in interpreting measurements at the energy and cosmic frontiers. We focus on the plans of the U.S. lattice QCD Collaboration (USQCD) for the next five years in this area. Companion documents, *Lattice Gauge Theories at the Energy Frontier*, *Lattice QCD for Cold Nuclear Physics*, and *Computational Challenges in QCD Thermodynamics*, address prospects in other areas of high-energy physics and nuclear physics for which lattice calculations are essential.

The methods of LQCD are now validated at the percent-level for a wide range of quantities, and have, over the last five years or so, obtained fully controlled results for about 20 hadronic matrix elements, with errors ranging from 0.5%–10%. Many of these results are essential in order to use existing experimental results to constrain the CKM parameters in the Standard Model (SM) and to search for physics beyond.

In the next five years, LQCD can play an expanded role in the search for new physics at the intensity frontier. We outline a program of calculations matched to experimental priorities, involving three main directions:

- We will calculate the new, more computationally demanding, matrix elements that are needed for the interpretation of planned (and in some cases old) experiments. These include the hadronic contributions to the muon $g - 2$, nucleon matrix elements for muon to electron conversion experiments, nucleon matrix elements for neutrino quasi-elastic scattering, long-distance contributions to kaon mixing and to $K \rightarrow \pi\nu\bar{\nu}$ decays, and the SM prediction for CP violation in $K \rightarrow \pi\pi$ decays (ϵ'). These require new methods, but the methodology is at a fairly advanced stage of development.
- We will steadily improve the calculation of the matrix elements needed for the CKM unitarity fit, most notably $B \rightarrow D^{(*)}$ form factors (needed for $|V_{cb}|$), $B \rightarrow \pi$ form factor (needed for $|V_{ub}|$), and B - \bar{B} mixing matrix elements. We forecast improvements by factors of 2–4 over the next five years, with most quantities having errors at or below the percent level. Key to achieving this will be the use of physical light quark masses. These improvements will significantly tighten the constraints on the SM, and provide better SM predictions for other rare processes.

We will also improve the determinations of the quark mass and the strong coupling constant to unprecedented accuracies. The bottom quark mass and α_s in particular will have important applications in high-precision Higgs studies at future colliders.

- At the accuracy we propose to obtain, we will need to include the effects of isospin breaking, electromagnetism, and dynamical charm quarks. We will thus need to re-validate our methods by comparing hadron masses to experiment, now with sub-percent accuracy.

To achieve these goals will require continued investment in hardware and software development, as well as the support of postdoctoral researchers and junior faculty.

II. INTRODUCTION

One of the foremost goals of high-energy physics is to test the Standard Model of particle physics (SM) and to search for indications of new physics beyond. Towards this aim, the experimental high-energy physics program is pursuing three complementary approaches: experiments at the “energy frontier” try to directly produce non-Standard Model particles in collisions at large center-of-mass energies; experiments at the “cosmic frontier” look for astronomical evidence of new interactions and aim to detect cosmically-produced non-SM particles through their interaction with ordinary matter; while experiments at the “intensity frontier” [1] make precise measurements of rare processes and look for discrepancies with the SM. Because intensity-frontier experiments probe quantum-mechanical loop effects, they can be sensitive to physics at higher energy scales than those directly accessible at the LHC, in some cases as high as 1,000 TeV or even 10,000 TeV [2]. Contributions from new heavy particles may be observable as deviations of the measurements from SM expectations, provided both the experimental measurements and theoretical predictions are sufficiently precise.

In many cases, and at all three frontiers, the SM predictions require calculations of hadronic properties such as decay constants, form factors, and meson-mixing matrix elements. These properties emerge at length scales where the underlying physics of quantum chromodynamics (QCD) is nonperturbative. Lattice gauge theory provides the only known method for *ab initio* results with controlled uncertainties, by casting the basic equations of QCD into a form amenable to high-performance computing. Thus, facilities for numerical LQCD are an essential theoretical adjunct to the experimental high-energy physics program: LQCD results are necessary for interpreting the results of many present and planned experiments as tests of the SM and searches for new physics.

During the past decade, the focus of many high-intensity experiments was the study of the quark-flavor sector. Heavy-flavor experiments such as BaBar, Belle, CDF, DØ, CLEO-*c*, and (more recently) BES III and LHC*b* established the oscillation of neutral B_s - and D -mesons, and made numerous measurements of decay branching fractions of B and D mesons, including the first measurements of leptonic B^+ - and B_s -meson decays. Much of the LQCD community effort over this same time period was therefore dedicated to calculating the corresponding hadronic matrix elements of operators in the electroweak effective Hamiltonian. Theoretical developments and increased computing power spawned a rapid maturation of LQCD calculations of electroweak matrix elements and ushered in the era of precision LQCD. With precise LQCD calculations available, heavy-flavor experiments measured the parameters of the Cabibbo-Kobayashi-Maskawa (CKM) quark-mixing matrix and established that the CKM paradigm of CP -violation describes experimental observations at the few-to-several-percent level. Thus LQCD played an important role in facilitating the quantitative comparison between theory and experiment that led to a share in the 2008 Nobel Prize in physics for Kobayashi and Maskawa. Continued progress in testing the Standard Model in the charm and bottom sectors will depend as much on improved LQCD calculations as on future super-flavor factories.

In the coming decade, applications of lattice QCD to the lepton-flavor sector will come to the forefront. The Muon $g - 2$ Experiment at Fermilab expects to reduce the uncertainty in the muon anomalous magnetic moment by a factor of four in the hope of definitively

confirming or refuting the current $\sim 3\sigma$ discrepancy between experiment and the SM. Muon-to-electron conversion experiments will require nucleon matrix elements from lattice QCD to interpret any observed new-physics signals in terms of underlying new-physics models. Neutrino experiments will require lattice QCD calculations to understand the Q^2 dependence of the key signal process, quasielastic neutrino-nucleon scattering. The quark-flavor effort will continue on several fronts: LHC***b*** and Belle II will measure the rates for many rare B -decays; NA62 at CERN plans to measure the $K^+ \rightarrow \pi^+ \nu \bar{\nu}$ branching fraction, while KOTO at J-PARC expects to see the first evidence for a nonzero $K_L \rightarrow \pi^0 \nu \bar{\nu}$ decay rate, and the proposed ORKA experiment at Fermilab and its successors aim to collect 1000 events or more in both channels. Other searches for BSM effects in hadron physics will require lattice calculations. Matrix elements with protons and neutrons are needed to interpret constraints on CP violation from limits on electric dipole moments, to aid the search for baryon-number violation in proton decay and neutron-antineutron oscillations, and even to guide searches for dark matter and axions at the cosmic frontier. Finally, future high-precision Higgs studies will require knowledge of the b quark mass to unprecedented accuracy. Therefore, the LQCD community must expand its program to meet the needs of these and other upcoming intensity-frontier experiments. In some cases, such as for many exclusive B -meson decay processes, improving the precision of existing calculations is sufficient, and the expected increase in computing power due to Moore's law will enable a continued reduction in errors. In other cases, such as for the muon $g - 2$ and the nucleonic probes of non-SM physics, new hadronic matrix elements are required; these new lattice calculations are typically computationally more demanding, and methods are under development.

This paper spells out the scientific priorities and plans for the next five years of the intensity-frontier thrust of the USQCD Collaboration's physics program. USQCD is an umbrella collaboration that aims to provide both the computational resources and software infrastructure for the lattice gauge theory research community in the United States. Support has been obtained from the high-energy physics and nuclear physics offices of DOE in the form of (i) funds for hardware and support staff, (ii) computational resources on leadership-class machines through INCITE awards, and (iii) SciDAC awards for software and algorithm development. The first has consisted of two 4–5 year grants, the second of which extends until 2014. Since its inception, the INCITE program has awarded computing resources to USQCD every year. SciDAC has funded four software projects for LQCD, the most recent beginning in 2012. All three components have been critical for progress in LQCD in the past decade, and in particular for the successful USQCD quark-flavor physics program. The primary purpose of USQCD is to support the high-energy and nuclear physics experimental programs in the US and worldwide. To this end, scientific priorities are established by the Collaboration and documented in white papers. USQCD's internal and INCITE computing resources are then allocated to self-directed smaller groups within USQCD to accomplish these goals.

This white paper is organized as follows. In Sec. III we summarize the dramatic progress in LQCD calculations in the past decade, with some emphasis on calculations carried out under the auspices of USQCD. We highlight calculations that validate the whole paradigm of numerical LQCD as well as those related to the intensity frontier, in particular flavor physics. This review sets the stage for Sec. IV, which breaks down our five-year outlook by physics topic: quark-flavor physics, charged-lepton processes, and nucleon matrix elements. Broadly, the LQCD intensity-frontier effort has two main thrusts: (i) improving the precision of present calculations and (ii) extending lattice methods to new quantities relevant for

upcoming experiments. Both require greater computational resources, and, where possible, we make forecasts for the expected lattice errors in five years based on the assumption that computing resources continue to increase according to Moore’s law and that funding to support postdocs and junior faculty in lattice gauge theory does not decrease. For the interested reader, two appendices provide more technical details that justify the forecasts presented in the main text. In Sec. V, we describe in some detail the computational resources needed to undertake the calculations discussed earlier. We summarize the case for continued support of the USQCD effort in Sec. VI.

The future success of the intensity-frontier program hinges on reliable SM predictions on the same time scale as the experiments and with commensurate uncertainties. Many of these SM predictions require nonperturbative hadronic matrix elements that can only be computed numerically with LQCD. The USQCD Collaboration is well-versed in the plans and needs of the experimental intensity-physics program over the next decade, and will continue to pursue the necessary supporting theoretical calculations. Implementation of the five-year program outlined in this white paper will require dedicated LQCD computing hardware, leadership-class computing, and efficient LQCD software. Therefore continued support of USQCD computing infrastructure and personnel is essential to fully capitalize on the enormous investments in the high-energy physics and nuclear-physics experimental programs. Indeed, LQCD calculations for the intensity frontier may play a key role in definitively establishing the presence of physics BSM and in determining its underlying structure.

III. CURRENT STATUS OF LATTICE QCD

In order to assess the prospects for future LQCD calculations, it is worthwhile recalling the huge strides made over the past decade or so. Much of this success stems from the increased support for LQCD infrastructure in the United States, as well as similar efforts in Japan, the UK, Germany, and Italy. We begin this section with a discussion of calculations that demonstrate the basic soundness of numerical LQCD. This work shows that lattice gauge theory has been able to reproduce hadron masses and decay amplitudes, even in cases where the correct result was not known in advance. We then provide a more detailed survey of quark flavor physics, because it most clearly illustrates the ideas behind the intensity-frontier program of the coming decade.

A. Validation of lattice QCD methodology

Although it lies outside intensity-frontier physics, the best place to start a discussion of the validation of LQCD methodology is the hadron spectrum. An *ab initio* understanding of hadron masses was one of the original attractions of LQCD. These masses are intrinsically interesting, because they are the origin of the mass of everyday objects. Figure 1 shows a summary of many hadron spectrum calculations, taken from a recent review [3]. These calculations encompass the light hadrons and also mesons with a heavy b or c quark bound to a light antiquark ($H^{(*)}$), strange antiquark ($H_s^{(*)}$), or each other ($\bar{b}c$ yields $B_c^{(*)}$). The

most striking feature of Fig. 1 is that so many calculations with different underlying details all agree well with experiment. Moreover, the mass of the nucleon, the source of everyday mass, has now been calculated with 1–2% accuracy. In addition, many calculations of the charmonium and bottomonium systems (not shown here) have obtained accurate results. Finally, the simplest decay matrix elements, f_π and f_K , have long agreed with the values in the Review of Particle Properties by the Particle Data Group (PDG), the most recent of which is Ref. [4].

Before expressing complete confidence in LQCD calculations for intensity-frontier applications, many particle physicists wanted to see genuine predictions, in contrast to the postdictions just discussed. In work enabled by the US DOE lattice infrastructure projects and their predecessors, USQCD groups have computed charmed-meson decay constants [8], semileptonic form factors [6], and the masses of the B_c [9] and η_b [10] mesons before being confirmed by measurements from experiments. As seen in Fig. 1, the prediction of the B_c^* meson mass awaits confirmation [11]. The charmed-meson semileptonic form factors are especially noteworthy, because they predict not only the normalization of the decay, but also the kinematic distribution, as shown in Fig. 2 with the most recent of several measurements.

Another noteworthy development of the past decade lies in the determination of the QCD coupling α_s and the quark masses. These quantities are the fundamental parameters of QCD, and the Lagrangian of lattice gauge theory contains free parameters corresponding to

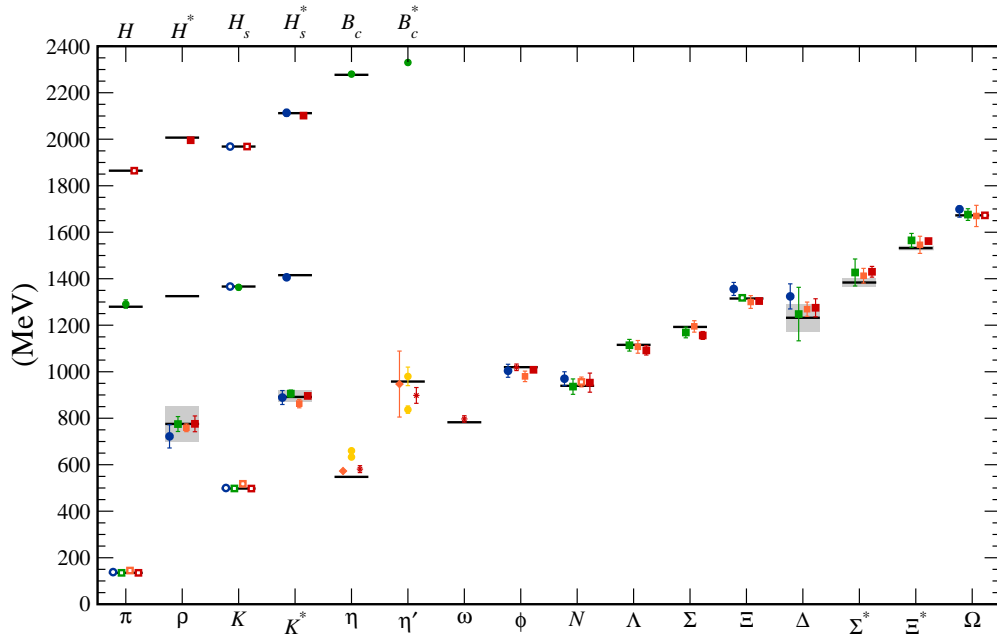


FIG. 1. Hadron spectrum from many different LQCD calculations. Open symbols denote masses used to fix bare parameters; closed symbols represent *ab initio* calculations. Horizontal black bars (gray boxes) show the experimentally measured masses (widths). b -flavored meson masses ($B_c^{(*)}$ and $H_{(s)}^{(*)}$ near 1300 MeV) are offset by -4000 MeV. Circles, squares and diamonds denote staggered, Wilson and domain-wall fermions, respectively. Asterisks represent anisotropic lattices ($a_t/a_s < 1$). Red, orange, yellow and green and blue signify increasing ensemble sizes (i.e. increasing range of lattice spacings and quark masses). For references, see Ref. [3].

each one of them. To fix these bare parameters, $1 + n_f$ hadronic quantities must be taken from experiment; this step is necessary and no different from any continuum formulation of QCD. Once the bare parameters are fixed, it is possible to convert them to renormalization schemes used in perturbative treatments of the SM.

The most recent PDG Review [4] contains a review of QCD [12], which incorporates five recent LQCD determinations of α_s [13–17]. The work of Refs. [13, 14, 17] is based on data generated under the auspices of USQCD, and has been thoroughly validated, in the sense discussed above of postdiction and prediction [18, 19]. The PDG review of QCD also surveys determinations of α_s from perturbative-QCD analyses of high-energy scattering experiments. It finds (in the $\overline{\text{MS}}$ scheme) [12]

$$\alpha_s(M_Z) = \begin{cases} 0.1185 \pm 0.0007, & \text{LQCD,} \\ 0.1183 \pm 0.0012, & \text{high-energy scattering,} \\ 0.1184 \pm 0.0007, & \text{combined.} \end{cases} \quad (1)$$

The current status, therefore, is that LQCD quotes errors that are competitive and, arguably, superior to those from perturbative QCD. More importantly, the LQCD and perturbative-QCD averages of α_s are in excellent agreement.

The most accurate determinations of the charmed and bottom quark masses come from studying moments of quarkonium correlation functions [17], which also yield α_s . These correlators provide an example of a class of methods in which LQCD is used to compute continuum-limit short-distance quantities that can then be compared with multi-loop continuum perturbative QCD calculations. In this case, parallel determinations using lattice results and experimental data are possible. The continuum perturbative calculations [20] can be matched either to LQCD results for correlators at spacelike momentum, or to e^+e^- annihilation data for correlators at timelike momentum. For $m_c(3 \text{ GeV})$ (in the $\overline{\text{MS}}$ scheme) the results are, respectively, $0.986(06) \text{ GeV}$ [17] and $0.986(13) \text{ GeV}$ [20]. For $m_b(10 \text{ GeV})$ the respective results are $3.617(25) \text{ GeV}$ [17] and $3.610(16) \text{ GeV}$ [20]. As with α_s , the agreement is striking, and together the two results bolster the notion that the QCD of hadrons is the same as the QCD of partons. A byproduct of this work is a precise ratio $m_c/m_s = 11.85(16)$ [21], which bootstraps the precise charmed quark mass to the light-quark sector.

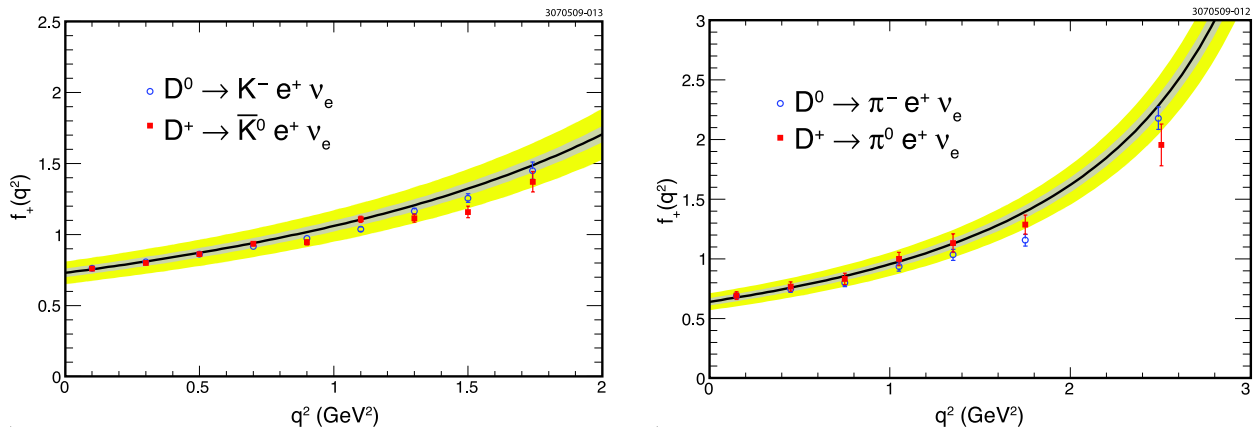


FIG. 2. Comparison [5] of $2 + 1$ LQCD calculations of D -meson form factors [6, 7] (curves with error bands) with measurements from CLEO [5] (points with error bars).

LQCD is the only way to determine the light-quark masses with any meaningful precision, so their determination does not validate lattice methods. Nevertheless, they are an important output of the last decade of LQCD research. Before LQCD brought the errors under control, the quoted uncertainty on the strange quark mass was approximately 30% and it was not clear whether the up quark mass was consistent with zero or not. Now several LQCD calculations have controlled most of the dominant uncertainties [19, 22–24]. The PDG review of quark masses [25] summarizes the overall uncertainties as 3%, 4%, and 7% for m_s , m_d , and m_u , respectively. In the broader context of particle physics, these results are interesting for several reasons. For example, in the SM, the quark-Higgs couplings are proportional to the masses. Furthermore, the nonzero value of m_u has implications for strong CP violation and motivates axion searches.

B. Quark flavor physics

We focus here on progress during the last five years, which is the period since our 2007 white paper on this topic [26]. This period has seen a rapid maturation of calculations of electroweak matrix elements. Five years ago, the era of precision lattice calculations was just beginning. Lattice methods had been validated at the few percent level for a range of spectroscopic quantities [26]. Accurate results were available for f_π (2.6% error) and f_K/f_π ($\sim 1\%$ error) using improved staggered fermions [27]. For quantities requiring matrix elements of four-fermion operators, e.g., B_K and $f_B^2 B_B$, and for heavy-quark decays, first unquenched calculations were available but some errors were not fully controlled. In addition, cross-checks from using multiple fermion discretizations were not yet available.

The present situation is greatly improved. Results with fully controlled errors are available for nearly 20 matrix elements, in almost all cases with multiple independent calculations. These quantities are the decay constants f_π , f_K , f_D , f_{D_s} , f_B and f_{B_s} , semileptonic form factors for $K \rightarrow \pi$, $D \rightarrow K$, $D \rightarrow \pi$, $B \rightarrow D$, $B \rightarrow D^*$, $B_s \rightarrow D_s$ and $B \rightarrow \pi$, and the four-fermion mixing matrix elements B_K , $f_B^2 B_B$ and $f_{B_s}^2 B_{B_s}$. Errors have been steadily reduced, such that sub-percent level is now possible for some quantities. One indication of the maturation of calculations is that it is now appropriate to perform world averages of lattice results, so as to provide the best input for phenomenological analyses [28, 29].¹

The amplitudes listed so far all have one hadron in the initial state and zero or one in the final state. They are especially straightforward to determine for several reasons. For example, the finite-volume errors are suppressed exponentially. Nonleptonic decays such as $K \rightarrow \pi\pi$ are more challenging: although the conceptual framework for computing these amplitudes has been available for twenty years, it was only in 2012 that the amplitude for $I = 2$ was brought under control [30, 31].

In Table I, we give examples of the status of LQCD calculations, comparing lattice errors in various matrix elements to those in the corresponding experimental measurements. Where available, we also include forecasts made in 2007 for the expected errors in ~ 2012 [26],

¹ The two averaging efforts have recently joined and expanded to form the worldwide “Flavor Lattice Averaging Group”, which plans to present updated averages on more extensive quantities in early 2013.

TABLE I. *History, status and future of selected LQCD calculations needed for the determination of CKM matrix elements. Forecasts from the 2007 white paper (where available) assumed computational resources of 10–50 TF years. Most present lattice results are taken from latticeaverages.org [28]. Other entries are discussed in the text. The quantity ξ is $f_{B_s}\sqrt{B_{B_s}}/(f_B\sqrt{B_B})$.*

Quantity	CKM element	Present expt. error	2007 forecast lattice error	Present lattice error	2018 lattice error
f_K/f_π	$ V_{us} $	0.2%	0.5%	0.5%	0.15%
$f_+^{K\pi}(0)$	$ V_{us} $	0.2%	–	0.5%	0.2%
f_D	$ V_{cd} $	4.3%	5%	2%	< 1%
f_{D_s}	$ V_{cs} $	2.1%	5%	2%	< 1%
$D \rightarrow \pi \ell \nu$	$ V_{cd} $	2.6%	–	4.4%	2%
$D \rightarrow K \ell \nu$	$ V_{cs} $	1.1%	–	2.5%	1%
$B \rightarrow D^* \ell \nu$	$ V_{cb} $	1.3%	–	1.8%	< 1%
$B \rightarrow \pi \ell \nu$	$ V_{ub} $	4.1%	–	8.7%	2%
f_B	$ V_{ub} $	9%	–	2.5%	< 1%
ξ	$ V_{ts}/V_{td} $	0.4%	2–4%	4%	< 1%
ΔM_s	$ V_{ts}V_{tb} ^2$	0.24%	7–12%	11%	5%
B_K	$\text{Im}(V_{td}^2)$	0.5%	3.5–6%	1.3%	< 1%

which have proven to be quite accurate. The forecasts shown for future improvements are discussed in Sec. IV and Appendix A.

It is important to note that, of the quantities in Table I, only for f_K/f_π was a result available in 2007 with all errors controlled. All other calculations have matured from having several errors uncontrolled to all errors controlled over the last five years. For $B \rightarrow D^{(*)}$ form factors and f_B , lattice errors are at, or below, the level of the corresponding experimental errors. USQCD calculations have played the major role in these reductions, and have solidified the error estimates by performing multiple calculations of several quantities using different fermion discretizations. For example, the world average for B_K is based on four different calculations, three of which were carried out under the auspices of USQCD.

These improvements have been possible because of a combination of the roughly 10-fold increase in computational resources, significant algorithmic improvements, and improved methods of theoretical analysis of the numerical data. The net effect has been that calculations have been possible with light-quark masses much closer to the physical values and with several lattice spacings and volumes to control discretization and finite-volume errors. Improved actions for domain-wall and staggered light quarks have reduced discretization errors. Smaller lattice spacings have allowed the use of relativistic charm quarks (rather than a heavy-quark action), increasing the precision in the charm sector, and enabling direct simulation of the charm sea.

On the theoretical side, a major advance has been the introduction of so-called SMOM renormalization schemes for applying nonperturbative renormalization (NPR) to bilinears [32] and four-fermion operators [33]. These schemes use non-exceptional momentum configurations, which significantly reduces long distance contributions to correlation functions, and so leads

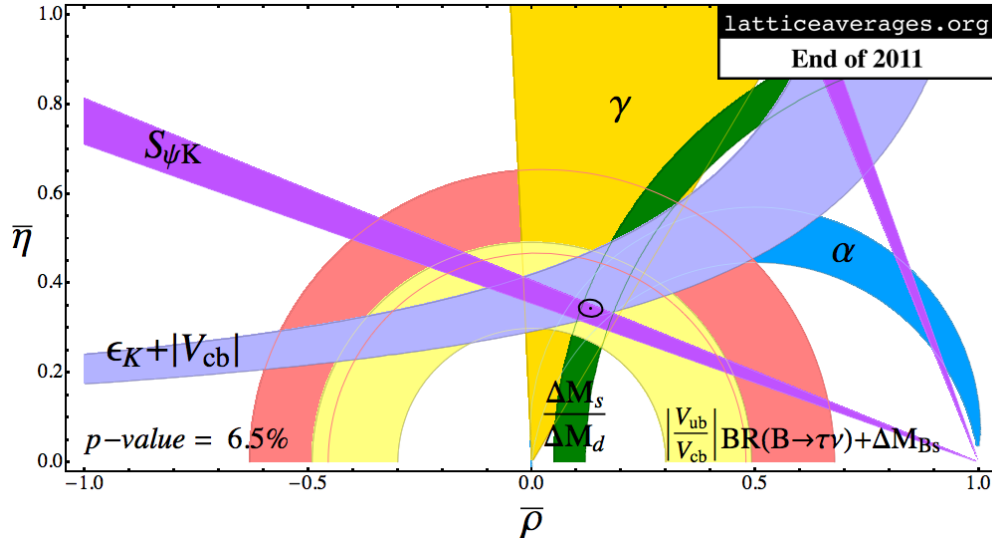


FIG. 3. Recent CKM unitarity triangle fit [35]. The resulting parameters are $\bar{\rho} = 0.136 \pm 0.017$, $\bar{\eta} = 0.349 \pm 0.012$ and $A = 0.821 \pm 0.014$. The constraints labeled $\epsilon_K + |V_{cb}|$ (light blue), $|V_{ub}/V_{cb}|$ (yellow), $\Delta M_s/\Delta M_d$ (green), and $BR(B \rightarrow \tau\nu) + \Delta M_{B_s}$ (pink) require lattice input, while the others ($S_{\psi K}$, α and γ) require minimal or non-lattice theoretical input. The solid ellipse encloses the 1σ region.

to smaller uncertainties in normalization factors for the operators. Similarly, the introduction of nonperturbative running (“step-scaling”) of operator normalizations has allowed the matching to continuum renormalization schemes to be done at higher momenta where perturbation theory (PT) is more reliable [34].

These improvements have, together with the extraordinary wealth of data from experiments, led to stringent tests of the CKM description of flavor physics and CP violation. First row unitarity (which relies on lattice results for f_K/f_π and the $K \rightarrow \pi\ell\nu$ form factor) is seen to hold at the part-per-mille level [29, 36]. The status of constraints on the CKM unitarity triangle is shown in Fig. 3. Overall, the CKM paradigm describes experimental observations at the few-percent level. While this is a triumph of the SM, the improved precision has unearthed a tension of around 3σ in unitarity fit, as shown in Fig. 3. A further long-standing disagreement of $\sim 3\sigma$ remains between the result for $|V_{ub}|$ determined from exclusive decays combined with lattice results and that from inclusive decays combined with the heavy-quark expansion.

C. Summary

The discussion in this section indicates the considerable advances in and successes of LQCD calculations over the last five years, but also highlights the need for further improvements. As Table I shows, for most quantities lattice errors are significantly larger than those in the corresponding experimental measurements. Thus LQCD remains the bottleneck in these cases, and, if we are to continue to squeeze the vise on the SM using flavor physics, we must

continue to reduce lattice errors. How this can be done is one of the two major topics in the following section, and Table I shows forecasts for the improvements that are possible.

In addition, there are several existing and many upcoming experiments that need various hadronic matrix elements in order to determine the SM “background” to new physics. Many of these require harder lattice calculations. Three examples of important matrix elements are (i) the long-distance contribution to the long-measured neutral kaon mass splitting, Δm_K , which can in principle provide a window onto new physics if we can calculate the SM contribution; (ii) the hadronic vacuum-polarization and light-by-light contributions to muon $g - 2$, which must be computed in order to allow the search for new physics from the upcoming experimental measurement at Fermilab; and (iii) nucleon matrix elements of a kind similar to the decay constants and form factors of mesons, which enter several arenas at the energy and cosmic frontiers. LQCD methods to support these experiments are either in hand or under active development. Discussion of these LQCD calculations forms the second major topic of the following section.

IV. FUTURE LATTICE CALCULATIONS

In this section we describe a broad program of LQCD calculations that will be possible over the next five years assuming that computer resources increase following Moore’s law. We have organized this program according to physics topic or class of experiments for which the calculations are needed. In each subsection, we explain the physics goals and their relationship to the experimental program, describe the status of present LQCD calculations, and explain what can be achieved over the next five years. Technical details providing detailed justification for future forecasts are provided in Appendices A and B.

While the challenges to further reductions in errors depend on the quantity, there are many common features. A key advance over the next five years will be the widespread simulation of physical u and d quark masses, obviating the need for chiral extrapolations. Such simulations have already been used for studies of the spectrum and several matrix elements with improved Wilson sea quarks [23, 37, 38]. USQCD is generating ensembles with physical masses for light sea quarks with highly-improved staggered quarks (HISQ) [39], domain-wall fermions (DWF) [40, 41], and improved Wilson fermions [42, 43]. Indeed, this effort is already well under way, as explained in Sec. V. These ensembles will also lead to reduced discretization errors compared to earlier ensembles (e.g., the MILC asqtad ensemble [19]) because the actions are more highly improved.

A second advance will be the systematic inclusion of isospin-breaking and electromagnetic (EM) effects. Once calculations attain percent-level accuracy, as is the case at present for quark masses, f_K/f_π , the $K \rightarrow \pi$ and $B \rightarrow D^*$ form factors, and \hat{B}_K , one must study the effects of EM and isospin breaking. A partial and approximate inclusion of such effects is already made for light quark masses, f_π , f_K and \hat{B}_K . Full inclusion would require nondegenerate u and d quarks and the incorporation of QED into the simulations. For some quantities it may suffice to implement this only for the valence quarks (quenched QED), while in general one must also include mass differences and electrical charges for the sea quarks. One approach for both isospin and unquenched QCD+QED simulations is to reweight pure QCD

configurations [44, 45]. One concern with QED is that the finite-volume effects will be enhanced due to the masslessness of the photon. In practice, to date, these effects seem to be controllable.

A final across-the-board improvement that will likely become standard in the next five years is the use of charmed sea quarks. These are included, for example, in the HISQ ensembles being presently generated. While it is expected that the error associated with quenching the charm quark is small for most quantities, this error is hard to estimate accurately without a direct lattice calculation.

A. Quark Flavor Physics

The present status of LQCD calculations related to quark flavor physics is summarized above in Sec. III B. Here we describe the future lattice calculations which will be needed to interpret past and future experiments, which are naturally categorized according to the nature of the lattice calculations. The first subsection discusses the “standard” matrix elements that have been our focus since 2007 [26] and are summarized in Sec. III B, where the challenge is to further reduce errors. Next we discuss lattice matrix elements needed for upcoming experiments which are of comparable difficulty to those already being calculated. Then we move to more challenging lattice calculations which are just now becoming possible and which should reach maturity in the next five years. Finally we mention yet more challenging quantities for which lattice methods are at an earlier stage of development.

1. *Standard lattice matrix elements*

Lattice-QCD calculations of matrix elements involving at most a single meson in both initial and final states are already at a mature stage. As discussed in Sec. III B, they are already playing an important role in flavor physics, because the methodology behind them is mature and widely understood. Nevertheless, in most cases lattice errors are larger than those in the corresponding experimental quantities, as shown in Table I. Thus, we can significantly tighten constraints on the SM by improving these calculations, with the aim of reducing, and ultimately removing, the gap between lattice and experimental errors. The forecasts in Table I indicate that we can achieve very significant improvements over the next five years.

These forecasts are based on detailed estimates of how the dominant errors in each quantity will be reduced by the expected increase in computing resources and known technical advances. Key improvements to all quantities come from the sources described above, particularly the use of physical quark masses, finer lattice spacings and improved lattice actions. In some quantities what is also needed is an improvement in the statistical errors, which will be achieved using the ensembles of larger lattices that are being generated. Improved methods of normalizing operators (in particular the SMOM scheme [32, 33]) will also play an important role.

In Appendix A we give a detailed, technical discussion explaining the forecasts for future errors given in Table I. Here we highlight those quantities where the improvements are

particularly important either for their potential to tighten the constraint on the SM or because of their connection with future experiments.

- **$B \rightarrow D^{(*)}$ form factors.** Lattice results for these form factors (particularly that for $B \rightarrow D^* \ell \nu$) allow for the determination of $|V_{cb}|$ from the measured decay rates. Uncertainty in $|V_{cb}|$ at present limits the strength of the constraint on the CKM unitarity triangle coming from ϵ_K . The error, which is magnified since it is $|V_{cb}|^4$ that enters, is much larger than the lattice error in the relevant matrix element, \hat{B}_K . The error in $|V_{cb}|$ also provides a major source of uncertainty in the SM prediction for $K \rightarrow \pi \nu \bar{\nu}$ (a process discussed further in Sec. IV A 3 below).

For the $B \rightarrow D^*$ form factor at zero recoil, the gap between experimental errors (1.3%) and lattice errors (presently $\sim 1.8\%$) has narrowed considerably over the last five years. In the next five years, we expect the lattice error to drop below the experimental error, as shown in Table I. Particularly important for this are the use of lattices with small lattice spacings and physical light-quark masses, and the extension of the calculation to nonzero recoil.

These form factors also provide examples of LQCD responding quickly to new experimental results by providing needed theoretical input. Most notable is the recent calculation by the Fermilab-MILC collaboration of the SM prediction for $R(D) = \text{BR}(B \rightarrow D\tau\nu)/\text{BR}(B \rightarrow D\ell\nu)$ with $\ell = e$ or μ [46]. Recent measurements of this quantity, and the analogous $R(D^*)$, differ from existing SM predictions (by 2σ and 2.7σ , respectively, for $R(D)$ and $R(D^*)$) [47]. Those SM predictions were based, however, on models of QCD, not *ab initio* QCD. Realizing that it was much easier to obtain accurate results for these ratios than for the form-factors themselves, the Fermilab-MILC collaboration responded quickly (using lattice data that were already in hand), and gave the first LQCD result for $R(D)$ [46]. Their result reduces the discrepancy with experiment to 1.7σ . At present, experimental errors ($\sim 16\%$) dominate over lattice errors (4.3%), so further lattice improvements are not needed in the short run. But in the longer term this situation may change, and should be straightforward to reduce the lattice error by a factor of 2 over the next five years.

- **$B \rightarrow \pi$ form factors.** These form factors provide the primary method of determining $|V_{ub}|$, and improvement is sorely needed. This is both because of the possibility of significantly tightening the unitarity constraint (by narrowing the light-yellow “ $|V_{ub}|/|V_{cb}|$ ” band in Fig. 3), but also because there is a long-standing disagreement between the lattice determination and that obtained using inclusive decays and the heavy-quark expansion. The discrepancy is about 3.6σ at present (see Appendix A for more details). The good news is that significant improvement is possible. While present lattice errors are about double those of experiment, we forecast a halving of the former by 2014 and a further halving by 2018. This improvement is due to a combination of all the factors noted above.
- **B -meson quantities.** Much of the improvement in calculations for quantities involving D -mesons in the last five years has been due to the use of improved actions and smaller lattice spacings. This allowed for relativistic charm quarks to be simulated, with automatically normalized vector and axial currents. In the next five years, increases in computational resources will allow us to move in a similar direction for

bottom quarks. Fully relativistic b -quarks are unlikely to be achieved until later, but, through extrapolation from somewhat lighter quarks, significant reductions in errors are possible. This is already the case for the HPQCD calculation of f_{B_s} using HISQ heavy quarks [48]. In addition, improved methods of simulating b -quarks at their physical mass, e.g., the nonperturbatively tuned clover action [49, 50] used in Ref. [51], will provide complementary information. Reductions in present errors for decay constants, form-factors and mixing matrix elements by a factor of 2 or more are forecast over the next five years.

- f_K/f_π and $f_+^{K\pi}(\mathbf{0})$. While these quantities are calculated with 0.5% errors, further improvement is needed to match experimental errors and tighten the test of unitarity from the first row of the CKM matrix. With errors this small, isospin breaking and EM effects must be considered. We forecast errors attaining the experimental level of 0.2% by 2018.
- Finally, we note that, for a few quantities, there is little impetus for improvement in the short term. Most notable is \hat{B}_K , where percent-level accuracy has been achieved through a concerted worldwide effort, with thorough cross checks.

2. Straightforward extensions of present calculations

There are a number of quantities where, by extending present methods, LQCD can provide matrix elements needed to constrain theories of new physics through their contributions to rare processes.

- **BSM contributions to K , D and B -meson mixing and $\Delta\Gamma_B$.** Flavor-changing neutral processes such as neutral meson mixing are suppressed in the SM. In BSM theories, by contrast, there is, generically, only kinematic suppression due to the heavy masses of new particles, and it is quite possible that BSM contributions are not that much smaller than those in the SM. Thus these processes provide a sensitive window into new physics. To provide detailed constraints on the models, however, one needs to know the matrix elements of four-fermion operators having all spin structures, since the left-handed nature of the weak interactions is not reproduced in general BSM theories.

For each of the K , D and B systems there are four new matrix elements in addition to those required in the SM. The required methodology and theoretical calculations are straightforward generalizations of those already undertaken. Results of comparable accuracy to those already obtained for the corresponding SM matrix elements (\hat{B}_K for kaons, $f_{B_s}^2 B_{B_s}$ for B_s -mesons, etc.) should be available by 2014. For the D case, which can be treated using relativistic quarks such as HISQ, we expect accuracy comparable to that for \hat{B}_K .

For B -mesons, there is an additional motivation for the calculation of the extra matrix elements, since two of them (for both B and B_s) enter into the leading order HQET expression for the width difference $\Delta\Gamma$ [52, 53].

Several calculations are already underway. For B -mesons, preliminary results are given in Ref. [54]. For kaons, results with $n_f = 2 + 1$ have been obtained with DWF [55] and staggered fermions [56], with other calculations underway.

- **$B \rightarrow K\ell^+\ell^-$ and related form factors.** This process can provide another sensitive window into new physics, but this requires accurate knowledge of the SM prediction. It is now well measured, and increasingly accurate results from LHC***b***, and eventually Belle II, are expected. The SM prediction requires knowledge of the vector and tensor $b \rightarrow s$ form factors across the kinematic range. Present theoretical estimates use light-cone sum rules, but several first-principles LQCD calculations are nearing completion, as reviewed in Ref. [57]. The calculation is similar to that needed for the semi-leptonic $B \rightarrow \pi$ form factor, and we expect similar accuracy to be obtained over the next five years.

A related process is the baryonic decay $\Lambda_b \rightarrow \Lambda\ell^+\ell^-$, recently measured by CDF. Here the extra spin degree of freedom can more easily distinguish between SM and BSM contributions. An LQCD calculation of the required form factors has recently been completed, using HQET to describe the b quark [58]. Errors of ~ 10 – 15% in the form factors are obtained, which are comparable to present experimental errors. The latter errors will decrease with new results from LHC***b***, and so improved LQCD calculations and cross-checks are needed. Although the calculation is conceptually similar to that for $B \rightarrow K\ell^+\ell^-$, given the presence of baryons we expect the errors for $\Lambda_b \rightarrow \Lambda\ell^+\ell^-$ to lag somewhat behind.

There are also experimental measurements of the closely related processes $B \rightarrow K^*\ell^+\ell^-$, $B \rightarrow K^*\gamma$ and $B_s \rightarrow \phi\gamma$. Lattice calculations of the required form factors are, however, not straightforward, since they involve a resonance in the final state. Such calculations actually become harder as one approaches physical quark masses, as the width of the K^* increases. They are of the “very challenging” type, examples of which are discussed below.

- **Non-SM form factors for $K \rightarrow \pi$, $B \rightarrow \pi$ and $B \rightarrow K$.** The $B \rightarrow K$ vector and tensor form factors just discussed are also needed to describe decays involving missing energy, $B \rightarrow KX$, in BSM theories [59]. Analogous form factors are needed for $B \rightarrow \pi X$ and $K \rightarrow \pi X$ decays [59]. The tensor form-factors are also needed to evaluate some BSM contributions to $K \rightarrow \pi\ell^+\ell^-$ [60]. Thus it is of interest to extend the present calculations of vector form factors in $K \rightarrow \pi$ and $B \rightarrow \pi$ to include the tensor matrix elements. Since these are straightforward generalizations of present calculations, we expect that comparable accuracy can be obtained quickly.

3. *More challenging calculations*

With recent advances in the methods of computational quantum field theory, numerical algorithms and computer technology, the weak interactions of the strange quark can be studied with increasing scope and precision. This opens exciting possibilities to pursue physics beyond the standard model because of beautiful and powerful experiments studying the decays and mixing of K mesons carried out over the past 40 years (in particular the NA48

and KTeV measurements of ϵ'/ϵ) as well as new experiments now underway or being actively planned. In contrast to the charm and bottom quarks, whose mass scales are sufficiently large that $O(m_q a)$ errors require careful attention, strange quarks are easily treated using standard lattice methods. Further, the relatively small mass of the kaon implies that decay final states are dominated by two pions, the case for which accurate theoretical control of QCD rescattering effects has been achieved [61, 62]. Initial results suggest that calculation of the two complex decay amplitudes A_0 and A_2 describing the decays $K \rightarrow (\pi\pi)_I$ for $I = 0$ and 2 respectively are now realistic targets for large-scale lattice QCD calculations. This would allow a verification of the $\Delta I = 1/2$ rule and a first-principles calculation of ϵ'/ϵ within the SM.

The $K \rightarrow \pi\pi$ amplitudes are dominated by first order weak processes in which a single W^\pm is exchanged. In the past, the only second order quantities that were accessible to LQCD were those which are dominated by short distances, e.g., the CP -violating parameter ϵ_K in K^0 - \bar{K}^0 mixing. These can be represented by matrix elements of local operators. However, roughly 5% of ϵ_K [63] and 30% of the K_L - K_S mass difference, ΔM_K , [64, 65] come from “long distances” in which the two flavor-changing interactions are separated by distances of order $\Lambda_{\text{QCD}}^{-1}$. Then both interactions, each represented by a four-fermion operator, must be explicitly included in a lattice calculation, a challenge which may now be possible to meet with present and near-future resources. Again, the effects of real intermediate states (rescattering effects) introduce finite-volume distortions. It has recently been demonstrated, however, that, in the case of kaons, these distortions can be corrected in a nonperturbative manner as part of the lattice calculation [66, 67].

The extension of lattice methods to second-order weak processes in general would have considerable impact on the search for new physics. Since the SM contributions are small, such processes are sensitive windows into new physics. This sensitivity would be enhanced were we able to predict the SM contributions accurately. One example is ΔM_K , but others for which lattice calculations may become possible are the decays $K^0 \rightarrow \pi^0 \nu \bar{\nu}$ and $K^+ \rightarrow \pi^+ l^+ l^-$. In particular, we note that new physics contributions to $K^0 \rightarrow \pi^0 \nu \bar{\nu}$ and $K^+ \rightarrow \pi^+ l^+ l^-$ are highly correlated with those to ϵ' , so that combining these processes will lead to much tighter constraints (see Ref. [68] and [talk](#) by U. Haisch [69]). We also stress that, at present, the $K^+ \rightarrow \pi^+ l^+ l^-$ decay is less favored experimentally because of the large uncertainty in the SM prediction. Were lattice calculations able to significantly reduce this uncertainty, this process would become of greater experimental interest.

We now give a brief summary of the future prospects for lattice calculations of the above-mentioned quantities. A more detailed discussion is given in Appendix B.

The complex $I = 2$ $K \rightarrow \pi\pi$ decay amplitude A_2 has now been computed using DWF with 15% errors [30, 31]. In the next two years, the addition of two smaller lattice spacings should reduce the dominant discretization error, leading to a total error of $\sim 5\%$. At this level, isospin violation must be included, which may be within reach on a five-year timescale. The $I = 0$ amplitude is considerably more challenging, with only trial calculations attempted to date [70]. As described in Appendix B, first physical results for A_0 with 15% errors are expected by 2014, and a 10% error appears possible by 2018. Since A_0 is the major source of uncertainty in ϵ' , similar errors are expected for that quantity.

The first second-order weak process to be tackled in detail will be ΔM_K . A method has been worked out in principle [66, 67], and there is a pilot numerical study [71–73]. The calculation

is more challenging than those for the $K \rightarrow \pi\pi$ amplitudes, with a key issue being the need to include dynamical charm quarks so as to enforce GIM cancellations. For a calculation at such an early stage in development, it is difficult to forecast the level of resources that will be required to obtain an accurate, controlled result. Pursuing this calculation will, however, be a major priority in the USQCD kaon program.

As methods are honed, the next step will be to extend the methods to calculations of the amplitudes for $K^+ \rightarrow \pi^+\nu\bar{\nu}$, $K_L \rightarrow \pi^0\nu\bar{\nu}$ and $K \rightarrow \pi\ell^+\ell^-$. The difficulties here are similar to those for ΔM_K , including the need for dynamical charm. We view these as a higher priority than studying the long-distance contribution to ϵ_K , in light of the ongoing NA62 experiment at CERN, the planned KOTO experiment at J-PARC, and opportunities for more sensitive measurements at Fermilab.

4. *Very challenging calculations*

In this subsection we briefly discuss several very interesting, but also very challenging, LQCD calculations on which progress may occur during the next five years. These concern CP violation in D decays, $D\bar{D}$ mixing, and light-cone distribution functions for B mesons. For these quantities the methodology is not yet mature, but some preliminary ideas have been suggested.

Recently, LHCb has presented evidence for CP violation in $D \rightarrow \pi\pi$ and $D \rightarrow K\bar{K}$ decays, since confirmed by CDF. The observed rate is larger than that predicted from the SM in various model calculations, and thus could indicate contributions from new physics. What is needed, however, is a reliable SM calculation; even a result with a large, but reliable, error would have a large impact. This need will become even more acute over the next five years as LHCb and Belle II improve the experimental measurement.

It is very challenging to reliably determine the SM prediction for such CP violation. In fact, the calculation is more challenging than that for $K \rightarrow \pi\pi$ decays, which, as discussed above, represent the present frontier of lattice calculations, with methods in place and first results just appearing.

We briefly describe the additional challenges faced in D decays. In the kaon case, one must deal with the fact that two-pion states in finite-volume are not asymptotic states, and the presence of multiple quark-disconnected contractions. For D decays, even when one has fixed the strong-interaction quantum numbers of a final state (say to $I = S = 0$), the strong interactions necessarily bring in multiple final states. For example, $\pi\pi$ and $K\bar{K}$ mix with $\eta\eta$, 4π , 6π , etc.. The finite-volume states used by lattice QCD are inevitably mixtures of all these possibilities, and one must learn how, in principle and in practice, to disentangle these states so as to obtain the desired matrix element. Recently, a first step towards developing a complete method has been taken [74], in which the problem has been solved in principle for any number of two-particle channels, and assuming that the scattering is dominantly S wave. This is encouraging, and it may be that this method will allow one to obtain semi-quantitative results for the amplitudes of interest. We expect that turning this method into practice will take 3–5 years due to a number of numerical challenges (in particular the need to calculate several energy levels with good accuracy). We also expect

that it will be possible to generalize the methodology to include four particle states; several groups are actively working on the theoretical issues. It is unclear at this stage, however, what time-scale one should assign to this endeavor.

Mixing occurs in the D - \bar{D} system, although there is no clear evidence yet for CP violation in this mixing [4]. As noted above, the short-distance contributions can be calculated for D mesons using LQCD, as for kaons and B -mesons. The challenge, however, is to calculate the long-distance contributions. As in the case of ΔM_K discussed above, there are two insertions of the weak Hamiltonian, with many allowed states propagating between them. The D system is much more challenging, however, since, as for the decay amplitudes, there are many strong-interaction channels having $E < m_D$. Further theoretical work is needed to develop a practical method.

The light-cone distribution function encodes the part of the Fock state wave function needed for high-energy exclusive processes, in particular nonleptonic B decays, such as $B \rightarrow K\pi$, $B \rightarrow \rho\rho$, etc. Moments of the distribution function can be expressed as hadron-to-vacuum matrix elements of local operators. The leading moment is proportional to the decay constant, and the first one or two nontrivial moments have been calculated for π , ρ , ϕ , K , and K^* with errors of order 10% for $n_f = 2$ [75] and $n_f = 2 + 1$ [76]. These results are already useful for B decays to these light mesons, and similar results for the moments of the B -meson distribution amplitude should be straightforward.

B. Charged lepton physics: Muon $g - 2$ and Mu2e

During the next five years, two important muon experiments will be mounted and carried out in the US. For one of them, a new measurement of the muon's anomalous magnetic moment, the largest theoretical uncertainties by far come from nonperturbative QCD. The other, a search for muon-to-electron conversion, aims to observe charged lepton-flavor violation for the first time. If successful, it would be evidence for a non-SM interaction, and lattice QCD calculations would be needed to interpret the nature of this interaction. Here, we discuss how lattice QCD relates to these two experiments.

1. Muon anomalous magnetic moment²

The muon anomalous magnetic moment provides one of the most precise tests of the Standard Model of particle physics (SM) and often places important constraints on new theories beyond the SM [1]. The current discrepancy between experiment and the Standard Model has been reported in the range of 2.9–3.6 standard deviations [77–79]. With new experiments planned at Fermilab (E989) and J-PARC (E34) that aim to improve on the current 0.54 ppm measurement at BNL [80] by at least a factor of 4, it will continue to play a central role in particle physics for the foreseeable future.

² This topic is also discussed in the companion white paper *Lattice QCD for Cold Nuclear Physics*.

Owing to the nonperturbative nature of QCD, the hadronic corrections to the muon $g-2$ are the largest source of error in the SM calculation. These errors must be reduced to leverage the new experiments [1]. The hadronic corrections enter at order α^2 through the hadronic vacuum polarization (HVP), shown in Fig. 4, and α^3 through hadronic light-by-light (HLbL) scattering, shown in Fig. 5, as well as higher order HVP contributions.

The HVP contribution to the muon anomaly has been precisely computed to an accuracy of 0.6% using experimental measurements of $e^+e^- \rightarrow$ hadrons and $\tau \rightarrow$ hadrons [78, 79]. The result including τ data is about 2 standard deviations larger than the pure e^+e^- contribution, and reduces the discrepancy with the Standard Model to 2.4 standard deviations [78]. The former requires isospin corrections which may not be under control. Alternatively, ρ - γ mixing may explain the difference and bring the τ -based result in line with that from e^+e^- [81]. LQCD calculations serve as an important independent check on these results, but at the moment statistical errors on lattice calculations of $a_\mu(\text{HVP})$ are at about the 3–5% level [82–87], and important systematic errors remain. Most significant is that, for light quark masses, the errors on the low-momentum region of $\Pi(Q^2)$ are not small enough, nor are there sufficient points available in the crucial region, $Q^2 \sim m_\mu^2$, to adequately estimate $a_\mu(\text{HVP})$. Quark masses are still too heavy (and errors are still too large for light masses), so fits are model-dependent. The good news is that all of these points are being addressed in the latest calculations. Lattice calculations using model independent fit functions [88], noise reduction techniques [89], twisted boundary conditions [87], charmed sea quarks [90], and physical light quark masses on large lattices are underway. Large error reductions over the next one to two years are not only possible, but likely. To get to the 1% level, or better, disconnected diagrams like the one shown on the right in Fig. 4 and isospin breaking effects must be incorporated to complete the calculation. At this level, the lattice QCD calculation becomes competitive with the traditional one based on e^+e^- and τ data, and may provide insight into the discrepancy between the two. Finally, we note that the HVP lattice calculation can be used to compute the QCD running of the fine structure constant, which plays

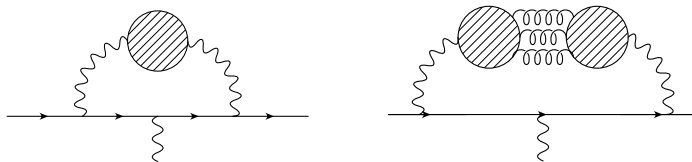


FIG. 4. Hadronic vacuum polarization diagrams contributing to the muon anomaly. The horizontal lines represent the muon. The blobs formed by the quark loops represent all possible hadronic intermediate states. Right panel: disconnected quark line contribution.

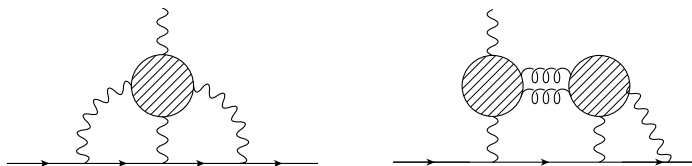


FIG. 5. Hadronic light-by-light scattering diagrams contributing to the muon anomaly. The horizontal lines represent the muon. The blobs formed by the quark loops represent all possible hadronic intermediate states. Right panel: one of the disconnected quark line contributions.

an important role in precision electroweak constraints of BSM theories.

The HLbL contribution to the muon anomaly cannot be computed using data from experiment and a dispersion relation as for the HVP contributions. Thus present estimates of this contribution use models, which have errors estimated in the 25-40% range [91, 92] (i.e. roughly half the size of the present error from the HVP). If not reduced, these errors will dominate over the HVP error as the latter is reduced (either from more experimental data, lattice calculations, or both). Thus there is a crucial need for an *ab initio* calculation, and the prior absence of such a calculation has been used as a reason not to do the new experiment. Fortunately, significant progress has been made on an *ab initio* method using LQCD, and the prospects for achieving a calculation with $\sim 20\%$ errors in the next five years are good, as we describe below. Assuming this, and a reduction of the HVP error by a factor of 2, and the expected reduction in experimental errors, then the present central value would lie $7\text{-}8\sigma$ from the SM prediction.

First LQCD results for the single quark loop part of the HLbL contribution (Fig. 5, left panel) have been reported recently [93]. The calculation is performed using a novel technique that combines both QED and QCD on the lattice in a single non-perturbative framework [94]. The method can be checked in pure QED, where the LbL term has been calculated directly in perturbation theory, allowing a benchmark for the procedure. This test was performed successfully in Ref. [95], showing the significant promise of the method. Much effort is still needed to reduce statistical errors, extrapolate to zero momentum transfer, and many systematic errors remain uncontrolled. However, first signs of the HLbL contribution rising above the Monte-Carlo noise are encouraging. The calculation is quenched with respect to QED, so the sea quarks are not charged, and potentially large contributions are missing (*i.e.*, diagrams like the one shown in the right panel of Fig 5). This can be fixed simply by using dynamical QCD+QED gauge configurations, or by reweighting the quenched ensembles. All of these approaches are under investigation.

Intermediate calculations are also being done, or considered, that will check both model and lattice calculations: for example, the $\pi^0 \rightarrow \gamma^{(*)}\gamma^{(*)}$ vertex function [96], the axial-vector–vector–vector three-point function [97], the chiral magnetic susceptibility [98], as well as the four-point vector correlation function in QCD needed for the HLbL amplitude, computed at select fiducial values of the momenta at each vertex. The first of these is also directly related to experimental measurements of the Primakoff effect, $\gamma A \rightarrow \gamma\gamma$, which is dominated (like HLbL) by the pion pole.

The goal, including lattice calculations, from the INT workshop on the HLbL contribution to the muon anomaly [99], was to reduce the HLbL error to 10% from the current model uncertainty of 25–40% by 2016–17. Reaching this milestone is possible with sustained effort on the lattice calculations and continued advances in computer power, but is not guaranteed.

2. Muon-to-electron conversion

In the Standard Model with neutrino masses and mixing, charged-lepton flavor violation is possible but suppressed by many factors, particularly the small splittings of neutrino mass eigenstates. Thus, any observation of $\mu N \rightarrow e N$, where N is a nucleus, or the related

process $\mu \rightarrow e\gamma$ would be an unambiguous sign of new physics. Many experiments searching for charged-lepton flavor violation are running or are on the horizon, motivated by pure exploration and models of new physics that suggest a measurable rate. The MEG experiment at PSI is currently searching for $\mu \rightarrow e\gamma$, and an improved search for $\mu \rightarrow eee$ at PSI (the Mu3e Experiment) has also been proposed. The Mu2e Experiment at Fermilab aims to improve the sensitivity to $\mu N \rightarrow eN$ by four orders of magnitude.

To interpret these experiments, especially if a discovery is made, lattice-QCD calculations are needed, because the theory requires knowledge of the light- and strange-quark contents of the nucleon [100, 101]. These are the matrix elements $\sigma_{\pi N} = \frac{1}{2}(m_u + m_d)\langle N | (\bar{u}u + \bar{d}d) | N \rangle$, $m_s\langle N | \bar{s}s | N \rangle$, and the ratio $\langle N | (\bar{u}u - \bar{d}d) | N \rangle / \langle N | (\bar{u}u + \bar{d}d) | N \rangle$. (Where N now denotes a nucleon.) The theory of μ -to- e conversion also requires vector matrix elements, replacing $m_q\bar{q}q$ with $\bar{q}\gamma^\mu q$, but these can be measured in electron scattering.

These matrix elements can be computed in lattice QCD, although correlation functions for nucleons are noisier than for meson, and the isoscalar contributions require disconnected diagrams. Many lattice collaborations have calculated the strange-quark content $m_s\langle N | \bar{s}s | N \rangle$ with $N_f = 2 + 1$ and even $N_f = 2 + 1 + 1$ flavors and several different fermion formulations [102–111]. The results obtained with different methods and lattice formulations agree at the 1–2 σ level. A recent compilation quotes an average value $m_s\langle N | \bar{s}s | N \rangle = 40 \pm 10$ MeV [111]. Thus, lattice-QCD results already rule out older estimates that suggested much larger values for $m_s\langle N | \bar{s}s | N \rangle$, as large as ~ 300 MeV. The more accurate lattice results are now replacing the older, cruder results which had previously been used in phenomenology [112].

Lattice-QCD can also provide first-principles calculations of the pion-nucleon sigma term $\sigma_{\pi N}$ [102, 104–106, 110] and the charm-quark content $m_c\langle N | \bar{c}c | N \rangle$ [109, 113]. A realistic goal for the next five years is to pin down the values of the quark scalar densities for $q = u, d, s, c$ with ~ 10 –20% uncertainties. Even greater precision can be expected on the timescale of a continuation of Mu2e, which would either reach for greater sensitivity or exploit different target nuclei to discriminate among models of new physics [101]. As discussed in Sec. IV C 4, the same nucleon matrix elements are also needed to interpret some dark-matter detection experiments [114–116].

C. Neutrino physics, underground physics, and related processes

Several aspects of particle physics require nucleon matrix elements [117], so we discuss the underlying physics and status of calculations here. Further aspects of nucleon properties, and, in particular, ongoing technical developments, are discussed in the companion white paper *Lattice QCD for Cold Nuclear Physics*. That white paper also contains material on LQCD calculations pertaining to nuclear forces, which will be needed to extract fundamental physics from nucleons in atomic nuclei.

1. Neutrino physics

The study of neutrino properties is a central part of particle physics. Future experiments, from the upcoming NOvA and MINOS+ to future projects such as LBNE and neutrino factories, have the potential to determine the mass hierarchy, to demonstrate the possible existence of sterile neutrinos, and to discover the magnitude of CP violation in the lepton sector.

Measurement of neutrino oscillation parameters, and the possible discovery of new neutrino states, is limited by our understanding of the cross section at accelerator energies. The basic signal process for $\nu_\mu \rightarrow \nu_e$ oscillations is charged-current quasielastic (CCQE) scattering on a bound neutron. It is described by the axial-vector form factor of the nucleon, $F_A(q^2)$, which is related to the matrix element $\langle p | \bar{u} \gamma^\mu \gamma^5 d | n \rangle$. Usually, the q^2 dependence is modeled by a dipole form [118]

$$F_A(q^2) = \frac{g_A}{(1 + q^2/m_A^2)^2}, \quad (2)$$

with the normalization g_A taken from neutron β decay. Unfortunately, this description is known to be inadequate in the related process of electron-nucleon scattering [119], so fits to this form are inevitably model dependent. Uncertainty in this form factor translates into an uncertainty of around 40% in the CCQE cross section [120–123]. Perhaps more alarmingly, different experiments are not in good agreement for m_A , when fitting to Eq. (2). The discrepancies could originate from nuclear effects in the target, but without an *ab initio* understanding of the nucleon-level form factor, one cannot know.

The shape of the axial-vector form factor $F_A(q^2)$ can be calculated from first principles by merging constraints from analyticity [124] with lattice QCD. This approach has been successful in quark flavor physics for $|V_{ub}|$ [125], as discussed above. Worldwide, the lattice-QCD community has a significant, ongoing effort devoted to calculating $F_A(Q^2)$ [126–129]. Until recently, results for the axial charge $g_A = F_A(0)$ have unfortunately not agreed well with neutron β decay experiments; see, e.g., Ref. [130] for a review. Now, however, two papers with careful attention to the chiral extrapolation and excited states [131] and with lattice data at physical up-down quark mass [132] find results in agreement with experiment, $g_A \approx 1.22$ – 1.24 . In addition to sensitivity to the chiral extrapolation, it is important to treat finite-volume effects more carefully than with mesons.

The current status of neutrino-nucleon scattering sets two interesting targets for the desired uncertainty in a lattice-QCD calculation of the form factor’s slope. On the one hand, Ref. [121] finds an (asymmetric) 12–25% uncertainty from fitting the MiniBooNE data to the model-independent z expansion. On the other, the (insufficiently justified) fits to the dipole form factor result in a putative 5% uncertainty. Refs. [131, 132] report total errors (apart from the omission of the strange and charmed sea) of a few per cent. Their work suggests that both phenomenologically relevant targets can be reached with the gauge-field ensembles described in Sec. V.

Also important for neutrino scattering is neutral-current elastic scattering. The physics issues run parallel to those discussed here, but now we must calculate an isoscalar matrix element with LQCD. The resulting disconnected diagrams make the calculations noisier and costlier, so (as with other isoscalar matrix elements) we forecast a more modest precision of $\sim 20\%$.

2. Baryon-number violation

Baryon-number violating processes, such as proton decay and neutron-antineutron mixing, are needed to generate the observed baryon asymmetry of the universe. Extended experimental searches have to date found no evidence for these processes, but future experiments aim to exclude greater regions of the parameter space suggested by extensions of the Standard Model. The interpretation of these measurements as tighter constraints on the models requires better knowledge of hadronic matrix elements, which LQCD can provide. They are of the standard type, differing only in that the operators involve three fermions and that one of the particles involved is a nucleon.

So far, there has been a small-scale effort devoted to calculating matrix elements for proton decay. Typical matrix elements are $\langle \pi | \mathcal{O} | p \rangle$, which is a key mode for water Cherenkov detectors, and $\langle K | \mathcal{O} | p \rangle$, which is a key mode for liquid-argon detectors. Here, \mathcal{O} is a three-quark operator. The only set of $n_f = 2 + 1$ calculations uses DWF [133], and quotes results for the relevant matrix elements with $\sim 20\text{--}40\%$ errors. It should be straightforward, with the larger ensembles now available and other improvements to reduce these errors to the $\sim 10\%$ level.

Another low-energy process that could provide distinct evidence for baryon number violation is the transition of neutrons to antineutrons, which violates baryon number by two units [134]. Experimentally, this can be searched for with large scale proton decay detectors such as Super-K [135] or LBNE, and also with experiments with nearly-free neutrons [136].

Initial work on these matrix elements is currently underway [137]. The main challenge at this stage is to obtain a statistically significant signal. We expect that a first result will be obtained in the next 1–2 years, with errors of $\sim 25\%$, and that results with errors of $\sim 10\%$ or smaller are achievable over the next five years. These calculations do not require disconnected diagrams, so we can ultimately expect very accurate results.

3. CP violation and electric dipole moments

Flavor physics experiments (aided, in part, by the lattice-QCD calculations described above) have demonstrated that SM CP violation is insufficient to explain the baryon asymmetry of the universe. Consequently, there must be as yet undiscovered CP -violating interactions beyond the SM. These could still show up in quark flavor-changing processes, but also elsewhere, such as in nonzero electric dipole moments of leptons and nucleons [138].

Electric dipole moments (EDMs) of fundamental particles are odd under time reversal, so the CPT theorem then implies that a nonzero value is a sign of CP violation. Searches for nonzero EDMs of leptons and nucleons are, thus, a promising way to search for BSM sources of CP violation [138]. We focus on the nucleon (free, or within nuclei), for which LQCD calculations are necessary [139]. In principle, there are three sources of a fundamental EDM. CKM CP violation makes a contribution to the nucleon EDM at the 3-loop level and lies well beyond experimental sensitivity. The strong CP -violating interaction, $\bar{\theta} G \tilde{G}$, directly makes a contribution to the nucleon, but not leptons. Finally, BSM sources of CP violation induce

EDM-generating higher-dimension operators. Interestingly, the strong- CP contribution flips sign between neutron and proton, while the BSM contributions need not flip sign.

LQCD calculations have been carried out for the matrix element needed for the strong- CP contribution to the neutron and proton EDMs [140], and those needed for BSM theories are underway [141]. This research is still in an early phase: once again disconnected diagrams are needed. A reasonable and useful goal for the coming five years is a suite of matrix elements with solid errors at the 10–20% level.

4. *Dark matter and other new interactions*

Searches for BSM contact interactions complement direct searches for new particles at the LHC. To infer (limits on) their properties, one requires a set of nucleonic matrix elements of the form $\langle N|\bar{q}\Gamma q|N\rangle$, where Γ encodes the spin structure. Examples include direct dark-matter detection, axion searches, and looking for new TeV-scale interactions with neutron β decay.

The cross section for detecting dark matter depends on how it interact with quarks inside the detector of CDMS, COUPP, etc. In many models, the interaction is spin independent, for example, if it is mediated by Higgs-boson exchange. In that case, the nucleon matrix elements $\sigma_{\pi N}$ and $m_s\langle N|\bar{s}s|N\rangle$ are needed to interpret the signal, just as for $\mu \rightarrow e$ conversion, discussed in Sec. IV B 2.

An example of spin-dependent dark matter is the axion, which couples to SM matter via the flavor singlet matrix element $\langle N|\bar{q}\gamma^\mu\gamma^5 q|N\rangle$. It is especially interesting, because its main motivation is to explain the strong CP problem. A first round of serious lattice-QCD calculations of $\langle N|\bar{q}\gamma^\mu\gamma^5 q|N\rangle$ has recently been carried out [108, 142, 143].

Finally, TeV-scale interactions, particularly those mediated by scalar and tensor exchange, can be probed with very precise measurements of neutron beta decay properties [144]. Here, the matrix elements $\langle p|\bar{u}d|n\rangle$ and $\langle p|\bar{u}\sigma_{\mu\nu}d|n\rangle$ must be computed. Because they are flavor nonsinglets, disconnected diagrams are not needed. These matrix elements are part of the program to study nucleon structure—see, e.g., Ref. [145]—and support experiments such as UCNA at LANL, Nab at the SNS, and PERC in Europe.

For all of these nucleon matrix elements, a goal for the next five years is to pin the values down to 10–20%. In all cases, such precision is sufficient for the time being. For example, lattice calculations of this accuracy for the nucleon scalar and tensor charges, combined with neutron decay, are more sensitive to scalar and tensor contact terms than a 25 fb^{-1} run at the 8 TeV LHC [146].

D. **Precision Higgs physics: improvements to quark masses and α_s**

As discussed in Sec. III, lattice QCD plays an important role in determining the basic parameters of QCD. The single largest source of error in the theoretical calculation of the

dominant Standard-Model Higgs decay mode $H \rightarrow b\bar{b}$ is the parametric uncertainty in the b -quark mass [147]. Because this mode dominates the total Higgs width, this uncertainty is also significant for most of the other Higgs branching fractions. Parametric uncertainties in α_s and m_c are the largest sources of uncertainty in the partial widths $H \rightarrow gg$ and $H \rightarrow c\bar{c}$, respectively. Future high-precision Higgs studies aim at measuring Higgs decay branching fractions to 1% or better. Since the width to the $b\bar{b}$ channel is proportional to δm_b^2 , in order that parametric uncertainty not dominate the understanding of this channel, $\delta m_b^2 \ll 0.5\%$ is needed. Currently, only LQCD offers a path to accomplishing this. Higgs physics is usually thought of as an Energy Frontier topic, but the high-precision Higgs studies envisioned here aim to search for small deviations from Standard-Model expectations. Thus they are more akin to Intensity Frontier studies than to Energy Frontier discovery studies, and they require the same type of high-precision LQCD calculations to support them.

The most precise known method for obtaining the quark masses m_c and m_b from lattice simulations employs correlation functions of quark currents [17, 148]. Moments of these correlation functions can easily be calculated nonperturbatively in lattice simulations and then compared to the perturbative expressions which are known to $\mathcal{O}(\alpha_s^3)$. Moments of the quark's electromagnetic current can also be determined from experimental e^+e^- -annihilation data as in Ref. [20]. The lattice determination of $m_c^{\overline{\text{MS}}}(m_c, n_f = 4) = 1.273(6)$ GeV is currently the most precise in the world [149]; this is primarily because the data for the lattice correlation functions is much cleaner than the e^+e^- annihilation data. The uncertainty is dominated by the estimate of neglected terms of $\mathcal{O}(\alpha_s^4)$ in the continuum perturbation theory. Therefore only modest improvements can be expected without a higher-order perturbative calculation.

The result for the b -quark mass obtained in this way is $m_b^{\overline{\text{MS}}}(m_b, n_f = 5) = 4.164(23)$ GeV [17], and is not currently as precise as the results from e^+e^- annihilation [20, 149]. The sources of systematic uncertainty are completely different than for m_c . In this case, perturbative uncertainties are tiny because $\alpha_s(m_b)^4 \ll \alpha_s(m_c)^4$, and discretization errors dominate the current uncertainty, followed by statistical errors. These should be straightforward to reduce by brute force computing power, and so are likely to come down by a factor of two in the next few years, perhaps to $\delta m_b \sim 0.011$ GeV or better. Precision of that order for m_b have already been claimed from e^+e^- data from reanalysis of the data and perturbation theory of Ref. [20], and coming lattice calculations will be able to check these using the computing power expected in the next few years.

The strong coupling constant, α_s , is also an output of these lattice calculations, and a very precise value of $\alpha_s(M_Z, n_f = 5) = 0.1183(7)$ has been obtained in Ref. [17], with an uncertainty dominated by continuum perturbation theory. Unlike the heavy-quark masses, for which the correlation function methods give the most precise results at present, there are numerous good ways of obtaining α_s with lattice methods [149]. Several other quantities have been used to make good determinations of α_s with LQCD, including Wilson loops [17], the Adler function [16], the Schrödinger functional [15], and the ghost-gluon vertex [150]. All of the lattice determinations are consistent, and each is individually more precise than the most precise determination that does not use LQCD. The most precise current determination of α_s may improve only modestly over the next few years, since its error is dominated by perturbation theory. However, the robustness of the global determination should improve as the precisions of the currently less precise determinations improve.

Lattice-QCD calculations have already determined the quark masses m_c and m_b and the

strong coupling α_s more precisely than is currently being assumed in discussions of Higgs decay channels [147]. The current uncertainties in α_s , m_c , and m_b from LQCD are all currently around a half a per cent and the results, especially for m_b , will continue to improve. For all of these quantities, increased corroboration from independent lattice calculations is expected in the next few years, making the determinations very robust. If the future lattice error on α_s is reduced by $\sim 30\%$ to ± 0.0004 , and that on m_b is reduced by a factor of two to ± 0.011 GeV, and these uncertainties are used in the Standard-Model Higgs predictions, then the parametric (total) uncertainty on $\Gamma(H \rightarrow b\bar{b})$ would be reduced to 0.8% (2.8%).

V. RESOURCES FOR STUDIES AT THE INTENSITY FRONTIER

In this section we discuss the computational resources needed to reach the scientific goals set out above. At present, members of USQCD are making use of dedicated hardware funded by the DOE through the LQCD-ext Computing Project, as well as a Cray XE/XK computer, and IBM Blue Gene/Q and Blue Gene/P computers, made available by the DOE's INCITE Program. During 2013, USQCD, as a whole, expects to sustain approximately 300 teraflop/s on these machines. USQCD has a PRAC grant for the development of code for the NSF's petascale computing facility, Blue Waters, and expects to obtain a significant allocation on this computer during 2013. Subgroups within USQCD also make use of computing facilities at the DOE's National Energy Research Scientific Computing Center (NERSC), the Lawrence Livermore National Laboratory (LLNL), and centers supported by the NSF's XSEDE Program. In addition, RBC Collaboration, has access to dedicated Blue Gene/Q computers at Brookhaven National Laboratory and the University of Edinburgh. For some time, the resources we have obtained have grown with a doubling time of approximately 1.5 years, consistent with Moore's law, and this growth rate will need to continue if we are to meet our scientific objectives. The software developed by USQCD under our SciDAC grant enables us to use a wide variety of architectures with very high efficiency, and it is critical that our software efforts continue at their current pace. Over time, the development of new algorithms has had at least as important an impact on our field as advances in hardware, and we expect this trend to continue, although the rate of algorithmic advances is not as smooth or easy to predict as that of hardware.

Lattice QCD calculations proceed in two steps. In the first, one performs Monte Carlo calculations to generate gauge field configurations with probability proportional to their weight in the Feynman path integrals of QCD. These configurations are saved, and in the second step of the calculations they are used to determine a variety of physical quantities. In order to obtain continuum QCD from lattice gauge theory, it is necessary to perform calculations at a variety of lattice spacings, and perform extrapolations to the limit of zero lattice spacing. Moreover, the computational resources required for the simulations increase as the masses of the quarks, the fundamental matter particles in QCD, decrease. Until recently it has not been possible to perform simulations with the two lightest quarks, the up and the down, at their physical masses. Instead, one carried out calculations with a range of heavier than physical up and down quark masses, and performed extrapolations to their physical values (chiral extrapolation). Supercomputers that have recently become available to lattice gauge theorists, such as the Blue Gene/Q and the Cray XE/XK are for the first time enabling us to carry out simulations with physical up and down quark masses at small

lattice spacings. This development will enable major advances on a range of important calculations.

Several different formulations of quarks on the lattice are currently in use by lattice gauge theorists. In our work at the intensity frontier, members of USQCD are currently focused on two of these: domain-wall fermions (DWF) [40, 41, 151], and highly improved staggered quarks (HISQ) [39]. Each of these formulations has its own advantages. Furthermore, in attempting to perform calculations with the precision at which we aim, it is very useful to employ more than one lattice formulation for at least some of the work in order to make certain that systematic errors are truly under control. We therefore discuss the computational resources needed for our calculations with both the DWF and HISQ actions in turn. In both cases we report the estimate of the total resource required in teraflop/s-years (TF years); one TF year is defined to be the number of floating point operations produced in a year by a computer sustaining one teraflop/s.

A. DWF resource requirements

1. Ensemble generation

Many quantities important to a search for physics beyond the standard model at the intensity frontier require accurate control of chiral symmetry to suppress unphysical operator mixing or to replicate the chiral structure of the standard model. Over the past fifteen years, the RBC collaboration, a subgroup of USQCD, together with their collaborators in the UK have developed the DWF formulation into a well understood tool, capable of accurately reproducing the chiral symmetries of QCD in a lattice calculation and allowing the physics of the up, down and strange quarks to be studied with percent level precision. The next generation of these calculations is now underway using physical values for the quark masses and $(6 \text{ fm})^3$ lattice volumes. Present ensemble generation is focused on lattice spacings of 0.11 and 0.086 fm, requiring lattice volumes of $48^3 \times 96$ and $64^3 \times 128$. These are listed as ensembles #1 and #2 in Table II. We anticipate completion of ensembles #1 and #2 by 2015 using resources at Argonne National Laboratory (ANL) and the University of Edinburgh. Shown as ensemble #3 in Table II is a less demanding, prototype, $32^3 \times 64$ ensemble generated at stronger coupling with G parity boundary conditions and somewhat smaller physical volume, but with larger statistics, that will be used to calculate $K \rightarrow \pi\pi$ decay into the $I = 0$ channel, the K_L-K_S mass difference ΔM_K , and certain rare kaon decays as discussed below. Similar small-volume ensembles at a sequence of decreasing lattice spacings will allow accurate nonperturbative matching between operators normalized at the $\mu \leq 3 \text{ GeV}$ scale accessible on ensembles #1 and #2 and those renormalized at 5–10 GeV where the errors in continuum QCD perturbation theory become increasingly controlled. It is likely that some of these specialized ensembles will also include a dynamical charm quark to provide nonperturbative information for matching renormalization factors between 2+1 and 2+1+1 flavor theories. These smaller ensembles will be generated using a combination of USQCD, RBRC and Edinburgh BG/Q computers in addition to INCITE resources. The next two ensembles, #4 and #5 listed in Table II, have parameters identical to #1 and #2, however electromagnetic effects have been included when generating the

TABLE II. Ensembles of gauge configurations to be generated with the domain wall (or related Möbius) fermion action. All ensembles with the exception of #3 have a physical extent of ≈ 6 fm in the spatial direction and ≈ 12 fm in the time direction. All have physical values for the quark masses. (Ensemble #3 has a spatial extent of 4.6 fm.) The number of floating point operations required to generate each ensemble is given in TF years in the final column. These estimates are based on current algorithms and methods and are thus may well turn out to be conservative in the light of future advances in technique. For reference, in one year a single BG/Q rack provides for such a calculation 50 TF years while the leadership class machines at LLNL and ANL contain 96 and 48 such racks respectively.

No.	N_f	a (fm)	$N_s^3 \times N_t$	Time units	TF years
#1	2+1	0.110	$48^3 \times 96$	5,000	175
#2	2+1	0.086	$64^3 \times 128$	5,000	390
#3	2+1	0.144	$32^3 \times 64$	10,000	44
#4	2+1+QED	0.110	$48^3 \times 96$	5,000	265
#5	2+1+QED	0.086	$64^3 \times 128$	5,000	585
#6	2+1	0.065	$96^3 \times 192$	3,000	1,400
#7	2+1+1	0.065	$96^3 \times 192$	3,000	1,400
#8	2+1+1	0.049	$128^3 \times 256$	3,000	5,700

ensembles. Following the exploratory calculations on ensemble #3 with G parity boundary conditions, we anticipate generating a third pair of ensembles, similar to #1 and #2 but with G parity boundary conditions. These are not listed in Table II but would require twice the resources of #1 and #2 and, if warranted by the $32^3 \times 64$ studies, would be used to increase the precision of the calculation of ϵ'/ϵ , ΔM_K and certain rare kaon decay predictions to the few percent level. Ensembles #6 and #7 in Table II have a smaller lattice spacing of 0.065 fm and are generated without and with a dynamical charm quark. The 2+1 flavor ensemble will provide a third lattice spacing, giving increased control of the continuum limit. It will also be critical to exploring the effects of charm quarks in kaon decay. If tests on smaller, less costly lattice volumes and further theoretical work indicate potentially important effects from charm quark loops, then a similar 2+1+1 flavor ensemble, #7, will also be generated. Finally, ensemble #8 also incorporates four flavors of quarks but at a second smaller 0.049 fm lattice spacing, allowing a continuum limit to be evaluated which includes the effects of dynamical charm quarks. (Even without dynamical charm quarks, a fourth ensemble with $a = 0.049$ fm would be needed to evaluate the continuum limit of results which include a valence charm quark.) These $96^3 \times 192$ and $128^3 \times 256$ chiral fermion ensembles, #6, #7 and #8, are too demanding to be generated with resources available today. They also require the development of evolution algorithms which remain ergodic at these small gauge couplings, a topic of active current research. However, we anticipate that these ensembles will be within the reach of the next generation of HPC machines with peak speeds of a few hundred petaflop/s, expected in 2016.

2. “Measurements”

A second critical topic when evaluating resource requirements is the increasing cost of calculating the multiple propagators and their contractions on these large lattice volumes with light quark masses, what are referred to a lattice QCD “measurements”. The computational cost of these measurements increases dramatically for calculation with physical quark masses for two reasons. The first is the familiar difficulty that comes from working with large lattice volumes and inverting a Dirac operator whose condition number increases as $1/m_{\text{quark}}$. The second is less familiar. For physical values of the up and down quark masses the kaon is composed of quarks with very different masses. This results in a kaon propagator which shows exponentially growing statistical fluctuations at increasing time separations, presenting noise which lies in severity between the nearly noise-free pion propagator and the extremely noisy propagator for the nucleon. These difficulties have spawned substantial advances in computational technique which are now dramatically changing the way these measurements are performed. Two recently developed strategies are effective for calculations with chiral fermions. The first, referred to as deflation, requires the calculation of a large number of eigenvectors with eigenvalues ≤ 100 MeV. At least 600 are needed for measurements on ensemble #1. The cost of this calculation can be amortized if many propagators are evaluated using the same set of low modes. The eigCG deflation algorithm [152] typically does this well. The second method, called all-mode-averaging (AMA) [89], uses inexpensive, approximate inversions, (typically with a conjugate gradient stopping condition between 10^{-3} and 10^{-4}) combined with a “fix-up” step which calculates a small correction for a subset of the measurements that can be applied to give an exact result. When applied to a challenging quantity such as a $q^2 = 0$, K_{l3} form factor, these techniques show as much as a twenty-fold increase in efficiency. For example, we estimate that a combined calculation of m_π , m_K , f_π , f_K , K_{l3} and A_2 (the amplitude for kaon decay into the $I = 2$, $\pi\pi$ state) on 100 configurations from ensemble #1 will require 55 TF years and yield the form factors in a calculation of K_{l3} with $\lesssim 0.3\%$ statistical errors. Such a calculation using deflation and AMA requires individual jobs which run for four days on one BG/Q rack, using the full 16 terabytes of machine memory. This example suggests that a full suite of calculations, possibly including those for ϵ'/ϵ , ΔM_K and rare kaon decays, may require resources that are in balance with those listed in Table II that are needed to generate the ensembles. However, these efficiencies can be realized only on leadership class machines where tens of sustained teraflop/s and tens of Terabytes of memory can be provided for a single job.

B. HISQ resource requirements

The MILC Collaboration, a subgroup of USQCD, is using the HISQ action to generate an extensive library of gauge configurations with four flavors of sea quarks: up, down, strange and charm. Like the ensembles generated earlier by this group with three flavors of improved staggered (asqtad [153, 154]) quarks [19], the HISQ ensembles are being made publicly available. They and the asqtad ensembles are being used by members of USQCD and others for a wide range of studies including precise calculations of standard model parameters, such as the gauge coupling constant and quark masses, and the weak interaction matrix elements needed for the determination of CKM matrix elements and tests of the standard model,

listed in Table I.

In the first phase of the HISQ configuration generation project, ensembles are being generated with four values of the lattice spacing in the range $a \approx 0.15$ fm to 0.06 fm in order to enable extrapolations to the continuum limit. At each of these lattice spacings, ensembles are being created with three values of the light quark mass, $m_l = (m_u + m_d)/2$, including the physical value. (Here m_u and m_d are the masses of the the up and down quarks). For these ensembles, the masses of the up and down quarks are taken to be equal, which has an effect of less than 1% on isospin averaged quantities, and the strange and charm quark masses are fixed at their physical values. All of the Phase 1 ensembles have been completed, or are nearing completion, except the one with $a \approx 0.06$ fm and physical quark masses. This is the most challenging staggered quark simulation undertaken to date, and it is only the advent of petascale computers, that make it feasible. We hope to complete this ensemble within the coming year, and then move on to ones with lattice spacings $a \approx 0.045$ fm and 0.03 fm in the future. These very fine grained ensembles will significantly increase the precision of all calculations performed with HISQ gauge configurations, and will have a particularly large impact on studies of b -physics, because they will, for the first time, enable use of staggered b -quarks. Until recently, b -quarks have been simulated using the Fermilab formulation of heavy quarks [155] or the nonrelativistic formulation of QCD (NRQCD) [156], both of which have leading lattice artifacts of order $O(a)$, whereas the asqtad and HISQ formulations have leading artifacts of order $O(a^2)$. However, we can only use HISQ valence quarks for lattice spacings such that $am_b < 1$, which is reached at $a \approx 0.03$ fm.

The masses and leptonic decay constants of light pseudoscalar mesons (π , K , D and D_s) are measured as the configurations are produced. These quantities are important in their own right, and they are used to monitor the runs and to determine the lattice spacing and sea-quark masses of the ensembles. The lattice spacing and sea-quark masses can only be estimated prior to the simulation. They are determined precisely through these measurement, which therefore impact all calculations performed with the configurations.

The resources required to generate HISQ gauge configurations with physical light, strange and charm quark masses, m_l , m_s and m_c , respectively, and to perform the pseudoscalar measurements, can be determined from our current runs with $a \approx 0.06$ fm, and the known scaling properties of our algorithms with lattice spacing, light-quark mass and lattice volume. They are given in the first three rows of Table III. These ensembles, like most generated earlier with the HISQ action have $m_u = m_d$. Ensembles with a heavier than physical value of m_l are also useful, but require a small fraction of the resources of the physical mass ones. Resources for ensembles with m_u and m_d fixed at their physical values, $m_u/m_d \approx 0.44$, are also shown in Table III. Those in rows four and five, like the $m_u = m_d$ ensembles, do not include the electromagnetic field, while those in rows six and seven do. As indicated above, configuration generation requires the most capable available supercomputers, whereas the pseudoscalar measurements, and a number of other measurement routines, can be run on large clusters with GPU accelerators, as well as on supercomputers.

In recent years, the resources spent on measurements other than the pseudoscalar ones described above, have been approximately four times those required to generate the configurations. This figure is growing in part because of the increasing sophistication of the measurements, and in part because of the expanding number of questions that can now be profitably addressed. The overwhelming fraction of resources for measurement routines go

TABLE III. Resources to generate gauge configuration ensembles with four flavors of HISQ quarks. The first column give the number of quark flavors with the notation 2+1+1 indicating that the masses of the up and down quarks are equal, and 1+1+1+1 that all four quark masses are unequal. The second column give the lattice spacing in fm, and the third column the ratio of up to down quark masses. In all ensembles, m_l , m_s , and m_c take on their physical values, whereas in the four with $m_u/m_d \approx 0.44$, the up and down quark masses are at their physical values as well. The fourth column gives the lattice dimensions, which are adjusted so that the spatial size of each box is fixed at 5.76 fm, and the temporal size at 11.52 fm. The fifth column gives the resources in TF tears to generate 6,000 molecular dynamics time units (1,000 equilibrated gauge configurations) for each ensemble, and the sixth column the resources to measure the properties of pseudoscalar mesons on these ensembles. These estimates are based on current algorithms and methods and are thus conservative.

N_f	a (fm)	m_u/m_d	$N_s^3 \times N_t$	Configuration generation (TF years)	Pseudoscalars measurements (TF years)
2+1+1	0.060	1.00	$96^3 \times 192$	14	24
2+1+1	0.045	1.00	$128^3 \times 256$	72	100
2+1+1	0.030	1.00	$192^3 \times 384$	650	760
1+1+1+1	0.060	0.44	$96^3 \times 192$	22	39
1+1+1+1	0.045	0.44	$128^3 \times 256$	120	160
1+1+1+1+QED	0.060	0.44	$96^3 \times 192$	32	56
1+1+1+1+QED	0.045	0.44	$128^3 \times 256$	170	240

into the inversion of the Dirac operator. Work is in progress on improved algorithms for this portion of the calculation, which could lead to a significant expansion in the scope of the physics that can be done with the HISQ ensembles. With present algorithms, we can generate the $a \approx 0.06$ fm and and 0.045 fm ensembles, and carry out a robust research program with them over the next three years, including work on all of the quantities listed in Table I. The $a \approx 0.03$ fm, physical quark mass ensemble will require the next generation of supercomputers expected in 2016.

VI. SUMMARY

Lattice QCD calculations now play an essential role in the search for new physics at the intensity frontier. They provide accurate results for many of the hadronic matrix elements needed to realize the potential of present experiments probing the physics of flavor. The methodology has been validated by comparison with a broad array of measured quantities, several of which had not been well measured in experiment when the first good lattice calculation became available. In the US, this effort has been supported in an essential way by hardware and software support provided to the USQCD Collaboration.

This document has laid out an ambitious five year vision for future LQCD calculations, explaining how they can provide essential and timely information for upcoming experiments

to test the Standard Model and search for physics beyond at the intensity, energy, and cosmic frontiers, by undertaking calculations of new, more computationally challenging, quantities. In addition, steady improvements in lattice results for matrix elements which are already well calculated will ensure that existing experimental results are fully utilized in the search for new physics. Our plans rely on continuing hardware and software support at similar levels to those of the last decade.

ACKNOWLEDGEMENTS

We gratefully acknowledge suggestions and comments from Marina Artuso, Brendan Casey, Tim Gershon, Richard Hill, Enrico Lunghi, Bob Tschirhart, and Jure Zupan.

Appendix A: Future prospects for standard weak matrix elements

In this Appendix we provide a more detailed discussion of the future prospects for the LQCD calculation of the “standard” matrix elements. These involve at most a single hadron in both initial and final states, and are the most advanced of the calculations discussed in this white paper. Calculations with all errors controlled have been done, in some cases with several results available using different fermion discretizations, and the challenge now is to reduce errors so that they drop below those coming from other sources. We explain here how we expect these errors to be reduced over the next five years, leading to the forecasts given in Table I.

1. First-row unitarity

Testing first-row unitarity of the CKM matrix requires the LQCD inputs f_K/f_π and $f_+(0)$ (the $K \rightarrow \pi$ semileptonic form factor at $q^2 = 0$). Present lattice results have achieved $\sim 0.5\%$ errors for both quantities, but this is still considerably larger than the 0.2% experimental errors. One should keep in mind, however, that these impressive-looking errors are somewhat misleading since the nontrivial part of the calculations is to obtain the differences from unity. These differences are ~ 0.2 and ~ -0.04 , for f_K/f_π and $f_+(0)$, respectively, so that the “true” lattice errors are closer to 2.5% and 10% . Seen in this light, the possibility of further improvement seems quite reasonable.

The ratio f_K/f_π has become a benchmark quantity, with consistent results obtained using asqtad, HISQ, DWF, and Wilson fermions. The present combined average is $f_K/f_\pi = 1.1936(53)$ [28] (0.44% error). This includes a correction from the isospin-limit lattice result to the physically relevant ratio f_{K^+}/f_{π^+} which is estimated to be -0.4% , i.e. comparable in size to the total error. Thus further improvement requires a reliable estimate of the error on this correction, which ultimately may require including isospin-breaking and QED effects (using the methods discussed in the main text).

The dominant error in the most accurate calculation (that of Ref. [157]), which uses the asqtad ensemble, comes from the chiral/continuum extrapolation. Presently this is ${}^{+0.3}_{-0.6}\%$. Moving to the presently available HISQ lattices with $a \approx 0.09$ and 0.12 fm and physical quark masses, should significantly reduce this error roughly to the level of the 0.2% statistical error. This leads to the total error estimate for 2014 of 0.3% given in Table I. Extending to the full planned HISQ ensemble with $a = 0.06$ fm physical quarks will reduce both statistical and systematic errors: we forecast a total error of 0.15% when combined with calculations using other fermions.

The situation for the $K \rightarrow \pi$ semileptonic form factor is less advanced. Until very recently, there was only one $n_f = 2 + 1$ calculation, using DWF and at a single lattice spacing [158]. There is now a second calculation, Ref. [36], using HISQ valence quarks on asqtad sea and two lattice spacing ($a = 0.09$ and 0.12 fm). There is also an $n_f = 2$ result using twisted-mass fermions with all errors controlled except for the quenching of the strange quark [159]. It is nevertheless included in world averages because the impact of quenching can be determined exactly at next-to-leading order (NLO) in chiral perturbation theory. Averaging the DWF

and twisted-mass calculations, `LatticeAverages.org` quotes $f_+(0) = 0.9584(44)$ [28], for a 0.46% total error. The very recent HISQ result, $f_+(0) = 0.9667(40)$ [36], has a slightly smaller error.

In the near future the DWF result will be fully controlled by the addition of a second lattice spacing. Combined with the updated valence HISQ results, an error of 0.35% in 2014 seems conservative. Before 2018, there should be results using valence and sea HISQ quarks with physical quark masses. Preliminary results at $a = 0.12$ fm find a 0.2% statistical error. Given that most systematic errors will be significantly reduced, as will statistical errors when the calculation is done on the entire HISQ ensemble, a total error of 0.2% seems attainable.

2. f_D and f_{D_s}

LQCD results for charmed meson decay constants are important both to provide methods for determining the CKM elements V_{cu} and V_{cs} , which allows a test of unitarity of the second row, and also as benchmark quantities for lattice calculations using charm quarks.

The LQCD calculations of these decay constants have improved much faster than forecast in the 2007 white paper. This is mainly due to the use of relativistic (HISQ) charm quarks, which makes the calculation comparable to that for f_K and f_π , and, in particular, fixes the normalization of the lattice axial currents. The most accurate results use HISQ valence quarks on asqtad sea, and find [160, 161]

$$f_D = 208.3(1.0)(3.3) \text{ MeV}, \quad f_{D_s} = 246.0(0.7)(3.5) \text{ MeV}. \quad (\text{A1})$$

Preliminary results using HISQ valence *and* sea quarks are in complete agreement [162]. The errors are slightly smaller than those in the present experimental measurements, and (using CKM elements from neutrino interactions and unitarity) the central values are consistent. The “ f_{D_s} puzzle” of a few years ago has thus disappeared as improved results have appeared (both experimental and lattice).

Combining the lattice f_D with the experimental $D^+ \rightarrow \mu^+ \nu$ decay rate now leads to the most accurate determination of $|V_{cd}|$, eclipsing those from semileptonic decays and neutrino interactions. On the other hand, combining f_{D_s} with the D_s leptonic decay rate leads to a less accurate determination of $|V_{cs}|$ than that from semileptonic decays (discussed below), although it provides an important cross check.

Experimental results for these decay constants will continue to improve, and thus it remains important to reduce lattice errors. These are likely not at the point where isospin breaking and EM effects in the sea need to be included, although valence isospin breaking is included in present lattice results. We expect a rough halving of lattice errors by 2014, since the present calculations will be extended to the full HISQ ensemble (including, in particular, physical light quarks at $a = 0.06$ fm). Further improvements beyond 2014 are hard to forecast in detail.

3. Semileptonic form factors for D decays

The $D \rightarrow \pi$ and $D \rightarrow K$ semileptonic form factors provide an alternative method for determining $|V_{cd}|$ and $|V_{cs}|$. As noted already, this method leads, at present, to the most accurate results for $|V_{cs}|$, while leptonic decays give a more accurate result for $|V_{cd}|$. Present experimental errors are significantly smaller than the lattice errors for both form factors (see Table I), providing strong motivation for improvements in the latter.

There is only one completed $n_f = 2 + 1$ lattice result, using HISQ valence quarks (for light and charm quarks) on asqtad sea (with $a = 0.09$ and 0.12 fm) [163, 164]. The results are

$$f_+^{D \rightarrow \pi}(0) = 0.666(20)(21) \quad \text{and} \quad f_+^{D \rightarrow K}(0) = 0.747(11)(15), \quad (\text{A2})$$

where errors are statistical and systematic, respectively. Results using ‘‘Fermilab’’ charm quarks [155] and asqtad light quarks (and with a down to 0.045 fm) are nearing completion and will have comparable errors [165]. This will provide an important check that the discretization of the charm quark is unimportant.

Over the next five years, calculations will be extended to the full set of HISQ ensembles, likely with HISQ valence quarks. Thus by 2018 chiral extrapolation errors should be removed, discretization errors at least halved (from the use of smaller a), and statistical errors reduced. We forecast a halving in the total errors by 2018, with intermediate errors at 2014. Thus by 2018 lattice errors should reach the level of (present) experimental errors.

4. Semileptonic $B \rightarrow D^{(*)}$ and $B_s \rightarrow D_s$ form factors

These form factors play an extremely important role in the CKM constraints since they determine $|V_{cb}|$. For example, the constraint from \hat{B}_K involves $|V_{cb}|^4$. Reducing the error in $|V_{cb}|$ is also important for other experiments searching for BSM physics (e.g., $K \rightarrow \pi \nu \bar{\nu}$) for which one needs to know the expected SM decay rate with good accuracy.

As shown in Table I, lattice errors are approaching those in present experiments. Nevertheless, given the importance of reducing errors in V_{cb} , it remains a high priority to further reduce the lattice errors to a level at or below those in experiments.

Since the experimental error in the $B \rightarrow D^*$ form factor is smaller than for $B \rightarrow D$, lattice calculations are presently concentrating on the former. The only $n_f = 2 + 1$ calculation uses the Fermilab approach for b and c quarks and asqtad light quarks (with $a = 0.06, 0.09$ and 0.12 fm). Combined with a somewhat old result from HFAG, one finds [28]

$$|V_{cb}|_{\text{excl}} = 39.7(0.7)_{\text{expt}}(0.7)_{\text{latt}} \times 10^{-3}. \quad (\text{A3})$$

This should be compared to the extraction using inclusive $b \rightarrow c$ semileptonic decays and using heavy-quark effective theory (HQET), which is [166]

$$|V_{cb}|_{\text{incl}} = 41.9(0.8). \quad (\text{A4})$$

Thus there is a small (1.7σ) discrepancy between inclusive and exclusive determinations. This provides further motivation to reduce lattice errors.

In the short term, a mild reduction in errors is possible by extending the calculation to the $a = 0.045$ fm lattices, which reduces discretization errors. Leaving other errors unchanged leads to the reduction from the present 1.8% to 1.5% as quoted in Table I. In the longer term, using the HISQ ensembles with physical quark masses will removed the chiral extrapolation error, leading to a total error below 1% (and thus below present experimental errors). In addition, the calculations are being extended to nonzero recoil [167], allowing comparison with experiment over a range of recoil momenta rather than just at the zero-recoil point. This will lead to smaller errors in $|V_{cb}|$.

Two recent calculations involving $b \rightarrow c$ form factors show how LQCD calculations have responded to new experimental results. For the last few years, experimental results for the ratio

$$R(D) = \frac{\text{BR}(B \rightarrow D\tau\nu)}{\text{BR}(B \rightarrow D\ell\nu)}, \quad (\ell = e \text{ or } \mu), \quad (\text{A5})$$

and the analogous quantity $R(D^*)$, have progressively improved. The best measurements are from BABAR, who find $R(D) = 0.440(58)(42)$ and $R(D^*) = 0.332(24)(18)$ [47]. These are, respectively, 2σ and 2.7σ above prior theoretical expectations in the SM. However, these expectations are not based on a first-principles calculations from QCD, which the lattice can now provide. The Fermilab-MILC collaboration have recently given the first LQCD result for $R(D)$ [46].

Since the $B \rightarrow D\tau\mu$ decay is not helicity suppressed, it is sensitive to both the vector and scalar form factors, $f_+(q^2)$ and $f_0(q^2)$. For decays to e and μ , by contrast, only the vector form factor enters. Thus a prediction for $R(D)$ requires knowledge of both of these form factors over the entire kinematic range. Although final results are not yet available for these $B \rightarrow D$ form factors, the calculation of ratios like $R(D)$ is more straightforward as many errors are reduced. Using only a subset of the asqtad ensemble, but working over a range of recoil momenta and using the z expansion, the Fermilab-MILC collaboration find $R(D) = 0.316(12)(7)$. This reduces the discrepancy with experiment down to 1.7σ .

At present, experimental errors ($\sim 16\%$) dominate over lattice errors (4.3%). In the future, it is likely that Belle II will reduce the experimental errors, and thus it may be worthwhile improving the lattice result. A significant improvement is, in fact, straightforward, since by extending the calculations to the full MILC set of asqtad ensembles, a reduction by 2 in both statistical and systematic errors seems possible. Thus we expect an error of $\sim 2.5\%$ by 2014. Errors could be further reduced by moving to the HISQ ensembles. The extension of the calculation to $R(D^*)$ is also underway.

The second new calculation is of the ratios

$$R_1 = f_0^{B_s \rightarrow D_s \ell \nu}(M_\pi^2)/f_0^{B \rightarrow D \ell \nu}(M_K^2) \quad \text{and} \quad R_2 = f_0^{B_s \rightarrow D_s \ell \nu}(M_\pi^2)/f_0^{B \rightarrow D \ell \nu}(M_\pi^2), \quad (\text{A6})$$

which involve the new form factor $B_s \rightarrow D_s$. These ratios are needed as part of an analysis to determine the ratio of b -quark fragmentation probabilities into B_s versus B_d . This in turn is needed at a hadronic collider as part of one of the methods used to extract the rate of the rare decay $B_s^0 \rightarrow \mu^+ \mu^-$. LHCb has recently obtained first evidence for this decay. Previous

results for R_1 and R_2 used QCD sum-rules, and found significant deviations from unity (i.e. from the U spin limit). The Fermilab-MILC collaboration, using only a subset of the asqtad ensemble, finds results consistent with U spin [168]:

$$R_1 = 1.046(44)(15), \quad \text{and} \quad R_2 = 1.054(47)(17), \quad (\text{A7})$$

At present, lattice errors are smaller than those coming from the experiments, but the latter will likely improve with further running at LHC**b**. Lattice errors, which are dominated by statistics at present, should improve substantially by extending the calculation to the full asqtad ensemble. We expect errors at the $\sim 2\%$ level by 2014.

5. $B \rightarrow \pi$ semileptonic form factor

This form factor provides the primary method for determining $|V_{ub}|$, the constraint on which plays a crucial role in the unitary triangle fits. LQCD provides results for the form factor for a range of q^2 , and compares with experiment using the z expansion. At present, this determination based on an exclusive $b \rightarrow u$ decay has a total error of 8.3%, $|V_{ub}|_{\text{excl}} = 3.12(26) \times 10^{-3}$, of which the lattice component is about twice that from experiment (see Table I).

There has been a longstanding discrepancy between this lattice-based result and that using inclusive decays and HQET: $|V_{ub}|_{\text{incl}} = 4.40(15)_{\text{exp}}(20)_{\text{th}}$ [166]. The discrepancy is about 3.6σ at present. Clearly it is crucial to reduce the lattice errors, both to pin down $|V_{ub}|$ more accurately, and to determine if the inclusive-exclusive difference is real.

There are at present two $n_f = 2 + 1$ calculations, both using the asqtad configurations with $a = 0.09$ and 0.12 fm, but differing in their treatment of the b quark. The HPQCD collaboration uses NRQCD [169], while the Fermilab-MILC collaboration uses the Fermilab approach [125]. The errors in the two calculations are comparable. Since these calculations are 4–6 years old, significant improvement is possible in the near term. Extending to the full asqtad ensemble will reduce statistical, chiral extrapolation and discretization errors, and a 4% total error in 2014 should be possible. This will match the present experimental error. In the longer term, extending the calculation to the HISQ ensembles with physical quark masses will plausibly reduce errors by another factor of 2.

There will also be results available in the next year or two using other methods: nonperturbatively tuned relativistic heavy quarks [49, 50] with DWF for the light quarks [51] and a lattice-HQET treatment [170].

HPQCD is also calculating related form-factors [171], in particular the $B_s \rightarrow K\ell\nu$ form factor which, combined with upcoming LHC**b** results, provides an alternative method to determine V_{ub} .

6. B -meson decay constants

f_B and f_{B_s} have long been benchmark quantities for LQCD calculations involving b -quarks. Indeed, several different methods for simulating the b -quark lead to consistent results, providing important validation of LQCD. In recent years, however, the decay constants have also

become important phenomenologically, determining $|V_{ub}|$ from the leptonic decay $B \rightarrow \tau\nu$, and solidifying the SM prediction for the recently measured decay $B_s \rightarrow \mu^+\mu^-$, a process which is very sensitive to new physics.

Combining $n_f = 2+1$ results from HPQCD [48, 172] and Fermilab-MILC [173], one finds [28]

$$f_B = 190.6(4.7)MeV, \quad f_{B_s} = 227.6(5.0)MeV, \quad f_{B_s}/f_B = 1.201(17), \quad (\text{A8})$$

which have errors of 2.5%, 2.2% and 1.4%, respectively. These errors should be compared to that in the experimental result for $\sqrt{\Gamma(B \rightarrow \tau\nu)}$, which is $\sim 9\%$ [166]. Thus, for this quantity, lattice calculations are likely to have smaller errors than experiment for some time to come. Note that the situation is reversed compared to the primary method for determining $|V_{ub}|$, the $B \rightarrow \pi$ form factor, where it is the lattice errors which are $\sim 9\%$, and larger than experimental errors.

Nevertheless, further improvements would be welcome for several reasons: (i) experiment errors in $\Gamma(B \rightarrow \tau\nu)$ will improve; (ii) it is important to further reduce the errors in the SM prediction for $B_s \rightarrow \mu^+\mu^-$; and (iii) because of the use of the decay constants as benchmarks for lattice calculations using b -quarks. Extending present calculations to the HISQ ensembles, including those at physical quark masses and $a = 0.06$ fm (or smaller), should allow gradual improvement down to the 1% level by 2018. In addition, calculations using the ‘‘ratio method’’ and relativistic twisted-mass quarks are underway [174], as are those using nonperturbatively tuned relativistic heavy quarks and light DWF [51], and using lattice HQET including $1/m_b$ corrections [175].

7. B -meson mixing matrix elements

B -meson mixing is now measured very accurately, with errors of 0.8% and 0.24% in ΔM_d and ΔM_s , respectively [166]. The lattice matrix elements needed to use these results are for $f_B^2 B_B$ and $f_{B_s}^2 B_{B_s}$, respectively. The smallest lattice errors result if one connects to experiment using $\xi = f_{B_s} \sqrt{B_{B_s}} / (f_B \sqrt{B_B}) \propto \sqrt{\Delta M_s / \Delta M_d}$ (for which the experimental error is 0.4%) and $f_{B_s}^2 B_{B_s} \propto \Delta M_s$. These two results play a very important role in the unitarity triangle constraint (see Fig. 3).

The required lattice matrix elements involve four-fermion operators, which are more complicated to calculate than most of the bilinear matrix elements discussed earlier in this section. Present $n_f = 2 + 1$ LQCD calculations are from HPQCD [176] and Fermilab-MILC [177], both using part of the asqtad ensembles ($a = 0.09$ and 0.12 fm), but differing in the choice of lattice b -quark (NRQCD for HPQCD and Fermilab formulation for Fermilab-MILC). They lead to a combined error of $\sim 4\%$ in ξ (adapted from Ref. [28] by the addition of an error due to ‘‘wrong taste-spin’’ operators [177]) and 11% in $f_{B_s}^2 B_{B_s}$ [28].

Thus there remains considerable room for improvement in the lattice calculations. Wrong taste-spin operators can be removed by fitting simultaneously to matrix elements of several four-fermion operators. The other dominant errors are from statistics, discretization, relativistic corrections (for NRQCD) and chiral extrapolation, all of which can be reduced by moving to the entire MILC asqtad ensemble. We estimate a combined error of 1.5% in ξ and

8% in $f_{B_s}^2 B_{B_s}$ in 2014. Moving to the HISQ ensemble, incorporating extrapolations from relativistic b quarks, and introducing other methods as for the decay constants, we forecast errors of $< 1\%$ and 5% , respectively, by 2018.

8. The kaon B parameter, \hat{B}_K

The final standard matrix element is \hat{B}_K . This describes the (dominant) short-distance part of CP violation in $K-\bar{K}$ mixing, and, plays an important, and complementary, role in the unitarity fits, as shown in Fig. 3. In the last five years, the lattice error has improved dramatically (far better than the 2007 forecast) due to a worldwide effort involving multiple types of fermions. The combined result is presently $\hat{B}_K = 0.7643(97)$ [28], with a total error of 1.3% . This combines $n_f = 2 + 1$ results with improved Wilson valence and sea [178] (the most accurate result to date), DWF valence and sea [179, 180], DWF valence on asqtad sea [181], and improved staggered on asqtad sea [182] (with the last three being done under USQCD auspices).

It is difficult to give an appropriate experimental error with which to compare the lattice error. On the one hand, the measurement of the quantity to which \hat{B}_K contributes, namely CP violation in kaon mixing (ϵ_K), has an error of 0.5% . This is the number appearing in Table I, and should be the ultimate goal of lattice calculations.

On the other hand, there are other errors which enter into the connection between \hat{B}_K and ϵ_K which are, at present, larger than that in \hat{B}_K . These are the perturbative truncation errors in Wilson coefficients (in particular in η_1 , the “charm-charm” coefficient) and the uncertainty in the long-distance contribution. In addition, to use B_K in the unitarity triangle fits (i.e. placing constraints on ρ and η) one needs $|V_{cb}^4|$, the present error in which is larger than any of the errors described above. The situation is illustrated by the *prediction* for \hat{B}_K obtained by performing the unitarity triangle fit *without including the LQCD input for \hat{B}_K* . The UTFIT web site quotes this as $\hat{B}_K = 0.85(9)$. Thus a lattice error $\ll 10\%$ is sufficient at present for the unitarity fit, a level of accuracy which has clearly been achieved.

Thus, in the short run, the B_K calculation is in very good shape. In the long run, however, it is worthwhile continuing to improve the calculation, as well as using it as a benchmark quantity for future lattice methods. The future forecasts in Table I are rather conservative (1% in 2014, from incremental improvements, and $< 1\%$ in 2018).

Appendix B: Future prospects for more challenging LQCD calculations

As described in the main text, advances in lattice methods and computational resources will allow the calculation of several new kaon properties over the next five years. In this Appendix we provide more technical details concerning likely progress.

1. $K \rightarrow \pi\pi$ amplitudes

For these amplitudes, The final state pions must have nonvanishing relative momenta so that their energy matches that of the initial kaon. For the $I = 2$ amplitude, A_2 , this can be achieved using appropriate boundary conditions on the valence quarks. It is also straightforward to work out the small (6%) finite volume (Lellouch-Lüscher) correction on the normalization of this state. Overall, the error is 15% [30, 31]. source of uncertainty comes from potentially large $O(a^2)$ errors since a single, rather large lattice spacing ($1/a = 1.36$ GeV) is used.

The error can be systematically reduced using smaller lattice spacings. A new calculation at $1/a = 1.73$ GeV using the Iwasaki gauge action has just begun with results expected in a year. A follow-up calculation with the same gauge action and a still finer lattice spacing ($1/a = 2.28$ GeV) will follow and yield $\approx 5\%$ error within perhaps two years. This would bring the result to the level at which the effects of isospin violation on the larger amplitude A_0 must be included.

The calculation of A_0 is much more difficult because of the overlap between the $I = 0$ $\pi\pi$ state and the vacuum, resulting in disconnected diagrams and a noise to signal ratio that grows exponentially with time. In addition, the simple boundary conditions used to give the ground state pions the necessary relative momentum cannot be used for $I = 0$, and G -parity boundary condition must be employed and imposed on both the valence and sea quarks. These topics have been actively pursued for a number of years and trial calculations carried out [70] to determine the best methods to suppress coupling to the vacuum. More than a factor of 10 improvement in statistics has been achieved and nonzero signals for both $\text{Re}A_0$ and $\text{Im}A_0$ have been observed for $K \rightarrow (\pi\pi)_{I=0}$ at threshold. Code has been written to generate 2+1 flavor gauge ensembles with G -parity boundary conditions [183]. However, a few more months of testing and additional coding effort are needed before the first full-QCD G -parity tests can be carried out. The first results for A_0 are expected within two years from a relatively coarse, $32^3 \times 64$ ensemble for an energy conserving decay with physical pion and kaon masses. Errors on ϵ' on the order of 15% will be achieved, with the dominant error coming from the finite lattice spacing. As in the case of the easier A_2 calculation, lessons learned from this first, physical calculation will then be applied to calculations using a pair of ensembles with two lattice spacings so that a continuum limit can be obtained. This second phase of the ϵ' calculation is less certain, requiring both success with the first, coarse lattice simulation and substantial additional resources beyond those listed in Table II. Ensembles #1 and #2 in Table II must be regenerated with G -parity boundary conditions imposed in all three spatial directions at twice the cost listed in Table II (since now the u and d quarks must be simulated independently). With some good fortune, this second phase of the calculation might be completed in five years and achieve errors on the 10% level. Here the largest source of systematic uncertainty arises from using 2+1 flavors and treating the charm quark using perturbation theory. Solutions to this problem which require using a still smaller lattice spacing and new methods to overcome the loss of ergodicity are now being actively studied. It is possible that only nonperturbative operator renormalization which explicitly includes the charm quark will be needed, in which case these charm quark effects will likely be incorporated within three years.

2. Long-distance contributions to ΔM_K

Promising techniques have been developed which allow the calculation of the long-distance contribution to ΔM_K by lattice methods. By evaluating a four-point function including operators which create and destroy the initial and final kaon and two effective weak four-quark operators, the required second order amplitude can be explicitly evaluated. Integrating the space-time positions of the two weak operators over a region of fixed time extent T and extracting the coefficient of the term which grows linearly with T gives precisely ΔM_K . Three problems must be overcome. First, the four-point function above includes terms which grow exponentially with T which must be subtracted. The statistical noise remaining after this subtraction gives even the connected diagrams the large-noise problems typical of disconnected diagrams. Preliminary results suggest that this problem can be solved by variance reduction methods and large statistics [73]. Second, finite volume effects must be removed by a careful treatment of intermediate $\pi\pi$ states degenerate with the kaon. This may not be difficult but has been inaccessible to the numerical experiments performed to date. Third, given the central importance of GIM cancellation in ΔM_K , a lattice calculation that is not burdened by multiple subtractions must include the charm quark mass. While apparently sensible results can be obtained even with $m_c a = 0.7$, believable systematic errors will require significantly smaller lattice spacing and an explicit continuum limit—a substantial challenge for a calculation which should also contain physical pions in an appropriately large physical volume. Perturbative results [64, 65] as well as the first lattice calculation [73] suggest that QCD perturbation theory works poorly at the energies as low as the charm mass, making the incorporation of charm in a lattice calculation a high priority here, as it is for the quantity $\text{Im}(A_0)$ entering ϵ' discussed above. Present results suggest that the first and second difficulties may be overcome in the next 2–3 years with the program outlined in this white paper, yielding results with all errors except those related to $m_c a$ effects controlled at the 10% level. Proper control of charm mass discretization errors may require the next generation of HPC machines and be five years away.

3. Long distance contributions to ϵ_K

The indirect CP violation parameter ϵ_K is closely related to ΔM_K discussed above, being essentially the imaginary part of the amplitude whose real part is ΔM_K . However, while ΔM_K is dominated by the contributions of u and c up-type quarks, even the long distance contribution to ϵ_K comes from amplitudes which contain u , c and t up-type quarks. Without the double GIM cancellation that makes the lattice calculation of ΔM_K convergent, the long distance part of ϵ_K will contain pieces of the form $\ln(m_{\text{charm}} a)$. These can be subtracted by standard Rome-Southampton techniques [73, 184] and replaced by quantities that can be computed accurately in perturbation theory, provided the subtraction energy is sufficiently large. While preliminary studies [71] suggest that such subtractions can be carried out successfully, the calculation of the $\approx 5\%$ long distance contribution to ϵ_K contains ingredients that are not present in ΔM_K . Thus, we believe it prudent to begin a calculation of the long distance part of ϵ_K after a realistic calculation of ΔM_K with 10% discretization errors has been completed, unless results in other areas increase the urgency with which a more accurate value of ϵ_K is needed.

4. Rare kaon decays

Given the promise of the first calculations of the long distance contributions to ΔM_K , a process that involves two W^\pm exchanges, it is natural to consider similar calculations for the second-order processes which enter important rare kaon decays such as $K_L^0 \rightarrow \pi^0 \ell^+ \ell^-$ or $K^+ \rightarrow \pi^+ \nu \bar{\nu}$. While in principle $K_L \rightarrow \ell^+ \ell^-$ should also be accessible to lattice methods, the appearance of three electroweak, hadronic vertices suggests that this and similar processes involving $H_W^{\Delta S=1}$ and two photons should be tackled only after success has been achieved with more accessible, second order processes.

The processes $K^+ \rightarrow \pi^+ \nu \bar{\nu}$ and $K_L \rightarrow \pi^0 \nu \bar{\nu}$ may be the most straightforward generalization of the current ΔM_K calculation. Here the dominant contribution comes from box and Z -penguin diagrams involving top quarks but with a 30% component of the CP -conserving process coming from the charm quark [185]. While the charm quark piece is traditionally referred to as “short distance”, the experience with ΔM_K described above suggest that a perturbative evaluation of this charm quark contribution may be unreliable and a lattice calculation, similar to that described for ΔM_K , may be essential if a 10% test of the standard model is to be performed. Given the on-going NA62 and KOTO experiments at CERN and J-PARC, this calculation might be given higher priority than the similar study of the long-distance contribution to ϵ_K .

The long distance contributions to the decay $K_{L/S} \rightarrow \pi^0 \ell^+ \ell^-$ also appear to be a natural target for a lattice QCD calculation.³ Here the CP -violating decay $K_L \rightarrow \pi^0 e^+ e^-$ may be of greatest interest and lattice QCD may provide a more accurate result, including the sign, for the indirect contribution by computing the CP -conserving process $K_S \rightarrow \pi^0 \ell^+ \ell^-$. While a similar approach to $K_L \rightarrow \pi^0 \mu^+ \mu^-$ could also be carried out, the results may be of less significance because of a two-photon, CP -conserving contribution which may be difficult to accurately estimate and is a more distant target for lattice QCD.

It should be emphasized that while USQCD and its UK collaborators have the human and computational resources to pursue this rare kaon decay topic, serious research has not yet begun so this discussion is necessarily preliminary and incomplete. We expect to begin pilot calculations within the coming year.

³ See recent [talk](#) of Chris Sachrajda [186].

-
- [1] J. L. Hewett *et al.*, *Fundamental Physics at the Intensity Frontier* (2012) arXiv:1205.2671 [hep-ex].
- [2] G. Isidori, Y. Nir, and G. Perez, *Annu. Rev. Nucl. Part. Sci.* **60**, 355 (2010), arXiv:1002.0900 [hep-ph].
- [3] A. S. Kronfeld, *Annu. Rev. Nucl. Part. Sci.* **62**, 265 (2012), arXiv:1203.1204 [hep-lat].
- [4] J. Beringer *et al.* (Particle Data Group), *Phys. Rev.* **D86**, 010001 (2012).
- [5] D. Besson *et al.* (CLEO), *Phys. Rev.* **D80**, 032005 (2009), arXiv:0906.2983 [hep-ex].
- [6] C. Aubin *et al.* (Fermilab Lattice, MILC, and HPQCD), *Phys. Rev. Lett.* **94**, 011601 (2005), arXiv:hep-ph/0408306 [hep-ph].
- [7] C. Bernard *et al.* (Fermilab Lattice and MILC), *Phys. Rev.* **D80**, 034026 (2009), arXiv:0906.2498 [hep-lat].
- [8] C. Aubin *et al.* (Fermilab Lattice, MILC, and HPQCD), *Phys. Rev. Lett.* **95**, 122002 (2005), arXiv:hep-lat/0506030 [hep-lat].
- [9] I. F. Allison *et al.* (HPQCD and Fermilab Lattice), *Phys. Rev. Lett.* **94**, 172001 (2005), arXiv:hep-lat/0411027.
- [10] A. Gray *et al.* (HPQCD), *Phys. Rev.* **D72**, 094507 (2005), arXiv:hep-lat/0507013.
- [11] E. B. Gregory *et al.* (HPQCD), *Phys. Rev. Lett.* **104**, 022001 (2010), arXiv:0909.4462 [hep-lat].
- [12] S. Bethke, G. Dissertori, and G. Salam (2012) in Ref. [4].
- [13] C. T. H. Davies *et al.* (HPQCD), *Phys. Rev.* **D78**, 114507 (2008), arXiv:0807.1687 [hep-lat].
- [14] K. Maltman, D. Leinweber, P. Moran, and A. Sternbeck, *Phys. Rev.* **D78**, 114504 (2008), arXiv:0807.2020 [hep-lat].
- [15] S. Aoki *et al.* (PACS-CS), *JHEP* **10**, 053 (2009), arXiv:0906.3906 [hep-lat].
- [16] E. Shintani *et al.* (JLQCD), *Phys. Rev.* **D82**, 074505 (2010), arXiv:1002.0371 [hep-lat].
- [17] C. McNeile, C. T. H. Davies, E. Follana, K. Hornbostel, and G. P. Lepage (HPQCD), *Phys. Rev.* **D82**, 034512 (2010), arXiv:1004.4285 [hep-lat].
- [18] C. T. H. Davies *et al.* (HPQCD, MILC, and Fermilab Lattice), *Phys. Rev. Lett.* **92**, 022001 (2004), arXiv:hep-lat/0304004.
- [19] A. Bazavov *et al.*, *Rev. Mod. Phys.* **82**, 1349 (2010), arXiv:0903.3598 [hep-lat].
- [20] K. G. Chetyrkin *et al.*, *Phys. Rev.* **D80**, 074010 (2009), arXiv:0907.2110 [hep-ph].
- [21] C. T. H. Davies *et al.* (HPQCD), *Phys. Rev. Lett.* **104**, 132003 (2010), arXiv:0910.3102 [hep-ph].
- [22] T. Blum *et al.*, *Phys. Rev.* **D82**, 094508 (2010), arXiv:1006.1311 [hep-lat].
- [23] S. Dürr *et al.* (BMW), *Phys. Lett.* **B701**, 265 (2011), arXiv:1011.2403 [hep-lat].
- [24] Y. Aoki *et al.* (RBC and UKQCD), *Phys. Rev.* **D83**, 074508 (2011), arXiv:1011.0892 [hep-lat].
- [25] A. Manohar and C. T. Sachrajda (2012) in Ref. [4].
- [26] R. Brower *et al.* (USQCD), www.usqcd.org (2007).
- [27] C. Bernard *et al.* (MILC), in *Chiral Dynamics 2006* (World Scientific, Singapore, 2008) arXiv:hep-lat/0611024 [hep-lat].
- [28] J. Laiho, E. Lunghi, and R. S. Van de Water, *Phys. Rev.* **D81**, 034503 (2010), updates at <http://latticeaverages.org/>, arXiv:0910.2928 [hep-ph].
- [29] G. Colangelo *et al.* (Flavianet Lattice Averaging Group), *Eur. Phys. J.* **C71**, 1695 (2011),

- arXiv:1011.4408 [hep-lat].
- [30] T. Blum *et al.* (RBC and UKQCD), Phys. Rev. Lett. **108**, 141601 (2012), arXiv:1111.1699 [hep-lat].
 - [31] T. Blum *et al.* (RBC and UKQCD), Phys. Rev. **D86**, 074513 (2012), arXiv:1206.5142 [hep-lat].
 - [32] C. Sturm *et al.*, Phys. Rev. **D80**, 014501 (2009), arXiv:0901.2599 [hep-ph].
 - [33] Y. Aoki *et al.*, Phys. Rev. **D84**, 014503 (2011), arXiv:1012.4178 [hep-lat].
 - [34] R. Arthur and P. A. Boyle (RBC and UKQCD), Phys. Rev. **D83**, 114511 (2011), arXiv:1006.0422 [hep-lat].
 - [35] J. Laiho, E. Lunghi, and R. Van de Water, PoS **LATTICE2011**, 018 (2011), arXiv:1204.0791 [hep-ph].
 - [36] A. Bazavov *et al.* (Fermilab Lattice and MILC), (2012), arXiv:1212.4993 [hep-lat].
 - [37] S. Aoki *et al.* (PACS-CS), Phys. Rev. **D81**, 074503 (2010), arXiv:0911.2561 [hep-lat].
 - [38] S. Dürr *et al.* (BMW), JHEP **1108**, 148 (2011), arXiv:1011.2711 [hep-lat].
 - [39] E. Follana *et al.* (HPQCD), Phys. Rev. **D75**, 054502 (2007), arXiv:hep-lat/0610092 [hep-lat].
 - [40] D. B. Kaplan, Phys. Lett. **B288**, 342 (1992), arXiv:hep-lat/9206013 [hep-lat].
 - [41] V. Furman and Y. Shamir, Nucl. Phys. **B439**, 54 (1995), arXiv:hep-lat/9405004 [hep-lat].
 - [42] M. Lüscher, S. Sint, R. Sommer, P. Weisz, and U. Wolff, Nucl. Phys. **B491**, 323 (1997), arXiv:hep-lat/9609035 [hep-lat].
 - [43] R. G. Edwards, B. Joó, and H.-W. Lin, Phys. Rev. **D78**, 054501 (2008), arXiv:0803.3960 [hep-lat].
 - [44] T. Ishikawa *et al.*, Phys. Rev. Lett. **109**, 072002 (2012), arXiv:1202.6018 [hep-lat].
 - [45] S. Aoki *et al.* (PACS-CS), Phys. Rev. **D86**, 034507 (2012), arXiv:1205.2961 [hep-lat].
 - [46] J. A. Bailey *et al.* (Fermilab Lattice and MILC), Phys. Rev. Lett. **109**, 071802 (2012), arXiv:1206.4992 [hep-ph].
 - [47] J. P. Lees *et al.* (BaBar), Phys. Rev. Lett. **109**, 101802 (2012), arXiv:1205.5442 [hep-ex].
 - [48] C. McNeile, C. T. H. Davies, E. Follana, K. Hornbostel, and G. P. Lepage, Phys. Rev. **D85**, 031503 (2012), arXiv:1110.4510 [hep-lat].
 - [49] N. H. Christ, M. Li, and H.-W. Lin, Phys. Rev. **D76**, 074505 (2007), arXiv:hep-lat/0608006 [hep-lat].
 - [50] H.-W. Lin and N. Christ, Phys. Rev. **D76**, 074506 (2007), arXiv:hep-lat/0608005 [hep-lat].
 - [51] O. Witzel, (2012), arXiv:1211.3180 [hep-lat].
 - [52] M. Beneke, G. Buchalla, and I. Dunietz, Phys. Rev. **D54**, 4419 (1996), arXiv:hep-ph/9605259 [hep-ph].
 - [53] A. Lenz and U. Nierste, JHEP **0706**, 072 (2007), arXiv:hep-ph/0612167 [hep-ph].
 - [54] E. D. Freeland *et al.* (Fermilab Lattice and MILC), (2012), arXiv:1212.5470 [hep-lat].
 - [55] P. A. Boyle, N. Garron, and R. J. Hudspith (RBC and UKQCD), Phys. Rev. **D86**, 054028 (2012), arXiv:1206.5737 [hep-lat].
 - [56] J. A. Bailey, T. Bae, Y.-C. Jang, H. Jeong, C. Jung, *et al.* (SWME), (2012), arXiv:1211.1101 [hep-lat].
 - [57] R. Zhou, (2013), arXiv:1301.0666 [hep-lat].
 - [58] W. Detmold, C.-J. D. Lin, S. Meinel, and M. Wingate, (2012), arXiv:1212.4827 [hep-lat].
 - [59] J. F. Kamenik and C. Smith, JHEP **1203**, 090 (2012), arXiv:1111.6402 [hep-ph].
 - [60] I. Baum, V. Lubicz, G. Martinelli, L. Orifici, and S. Simula, Phys. Rev. **D84**, 074503 (2011), arXiv:1108.1021 [hep-lat].
 - [61] M. Lüscher, Commun. Math. Phys. **105**, 153 (1986).

- [62] L. Lellouch and M. Lüscher, Commun. Math. Phys. **219**, 31 (2001), hep-lat/0003023.
- [63] A. J. Buras, D. Guadagnoli, and G. Isidori, Phys. Lett. **B688**, 309 (2010), arXiv:1002.3612 [hep-ph].
- [64] S. Herrlich and U. Nierste, Nucl. Phys. **B419**, 292 (1994), arXiv:hep-ph/9310311.
- [65] J. Brod and M. Gorbahn, Phys. Rev. **D82**, 094026 (2010), arXiv:1007.0684 [hep-ph].
- [66] N. H. Christ (RBC and UKQCD), PoS **LATTICE2010**, 300 (2010), arXiv:1012.6034 [hep-lat].
- [67] N. H. Christ (RBC and UKQCD), PoS **LATTICE2011**, 277 (2011), arXiv:1201.2065 [hep-lat].
- [68] M. Bauer, S. Casagrande, U. Haisch, and M. Neubert, JHEP **1009**, 017 (2010), arXiv:0912.1625 [hep-ph].
- [69] U. Haisch (Fermilab, June 14-23, 2012) talk at Project X Physics Study.
- [70] T. Blum *et al.* (RBC and UKQCD), Phys. Rev. **D84**, 114503 (2011), arXiv:1106.2714 [hep-lat].
- [71] J. Yu, PoS **LATTICE2011**, 297 (2011), arXiv:1111.6953 [hep-lat].
- [72] J. Yu (RBC and UKQCD), PoS **LAT2012**, 129 (2012).
- [73] N. H. Christ, T. Izubuchi, C. T. Sachrajda, A. Soni, and J. Yu (RBC and UKQCD), (2012), arXiv:1212.5931 [hep-lat].
- [74] M. T. Hansen and S. R. Sharpe, Phys. Rev. **D86**, 016007 (2012), arXiv:1204.0826 [hep-lat].
- [75] V. M. Braun *et al.* (QCDSF), Phys. Rev. **D74**, 074501 (2006), arXiv:hep-lat/0606012 [hep-lat].
- [76] R. Arthur *et al.* (RBC and UKQCD), Phys. Rev. **D83**, 074505 (2011), arXiv:1011.5906 [hep-lat].
- [77] T. Aoyama, M. Hayakawa, T. Kinoshita, and M. Nio, Phys. Rev. Lett. **109**, 111808 (2012), arXiv:1205.5370 [hep-ph].
- [78] M. Davier, A. Höcker, B. Malaescu, and Z. Zhang, Eur. Phys. J. **C71**, 1515 (2011), arXiv:1010.4180 [hep-ph].
- [79] K. Hagiwara, R. Liao, A. D. Martin, D. Nomura, and T. Teubner, J. Phys. **G38**, 085003 (2011), arXiv:1105.3149 [hep-ph].
- [80] G. W. Bennett *et al.* (Muon $g - 2$), Phys. Rev. **D73**, 072003 (2006), arXiv:hep-ex/0602035.
- [81] F. Jegerlehner and R. Szafron, Eur. Phys. J. **C71**, 1632 (2011), arXiv:1101.2872 [hep-ph].
- [82] T. Blum, Phys. Rev. Lett. **91**, 052001 (2003), arXiv:hep-lat/0212018.
- [83] M. Göckeler *et al.* (QCDSF), Nucl. Phys. **B688**, 135 (2004), arXiv:hep-lat/0312032.
- [84] C. Aubin and T. Blum, Phys. Rev. **D75**, 114502 (2007), arXiv:hep-lat/0608011.
- [85] X. Feng, K. Jansen, M. Petschlies, and D. B. Renner (ETM), Phys. Rev. Lett. **107**, 081802 (2011), arXiv:1103.4818 [hep-lat].
- [86] P. Boyle, L. Del Debbio, E. Kerrane, and J. Zanotti, Phys. Rev. **D85**, 074504 (2012), arXiv:1107.1497 [hep-lat].
- [87] M. Della Morte, B. Jäger, A. Jüttner, and H. Wittig, JHEP **1203**, 055 (2012), arXiv:1112.2894 [hep-lat].
- [88] C. Aubin, T. Blum, M. Golterman, and S. Peris, Phys. Rev. **D86**, 054509 (2012), arXiv:1205.3695 [hep-lat].
- [89] T. Blum, T. Izubuchi, and E. Shintani, (2012), arXiv:1208.4349 [hep-lat].
- [90] F. Burger, X. Feng, G. Hotzel, K. Jansen, M. Petschlies, *et al.*, (2013), arXiv:1308.4327 [hep-lat].
- [91] J. Prades, E. de Rafael, and A. Vainshtein, (2009), arXiv:0901.0306 [hep-ph].

- [92] A. Nyffeler, Phys. Rev. **D79**, 073012 (2009), arXiv:0901.1172 [hep-ph].
- [93] T. Blum, M. Hayakawa, and T. Izubuchi, PoS **LATTICE2012**, 022 (2012), arXiv:1301.2607 [hep-lat].
- [94] M. Hayakawa, T. Blum, T. Izubuchi, and N. Yamada, PoS **LAT2005**, 353 (2006), arXiv:hep-lat/0509016.
- [95] S. Chowdhury, (Ph.D. thesis, University of Connecticut 2009).
- [96] X. Feng *et al.*, Phys. Rev. Lett. **109**, 182001 (2012), arXiv:1206.1375 [hep-lat].
- [97] K. Melnikov and A. Vainshtein, Phys. Rev. **D70**, 113006 (2004), arXiv:hep-ph/0312226 [hep-ph].
- [98] B. L. Ioffe, V. S. Fadin, and L. N. Lipatov, *Quantum chromodynamics: Perturbative and nonperturbative aspects* (Cambridge University, Cambridge, UK, 2010).
- [99] Institute for Nuclear Theory Workshop (February 28–March 4, 2011).
- [100] T. Kosmas and J. Vergados, Phys.Rept. **264**, 251 (1996), arXiv:nucl-th/9408011 [nucl-th].
- [101] V. Cirigliano, R. Kitano, Y. Okada, and P. Tuzon, Phys. Rev. **D80**, 013002 (2009), arXiv:0904.0957 [hep-ph].
- [102] R. D. Young and A. W. Thomas, Phys. Rev. **D81**, 014503 (2010), arXiv:0901.3310 [hep-lat].
- [103] D. Toussaint and W. Freeman (MILC), Phys. Rev. Lett. **103**, 122002 (2009), arXiv:0905.2432 [hep-lat].
- [104] S. Dürer *et al.* (BMW Collaboration), Phys. Rev. **D85**, 014509 (2012), arXiv:1109.4265 [hep-lat].
- [105] R. Horsley *et al.* (QCDSF and UKQCD Collaborations), Phys. Rev. **D85**, 034506 (2012), arXiv:1110.4971 [hep-lat].
- [106] S. Dinter *et al.* (ETM Collaboration), JHEP **1208**, 037 (2012), arXiv:1202.1480 [hep-lat].
- [107] H. Ohki *et al.* (JLQCD Collaboration), Phys. Rev. **D87**, 034509 (2013), arXiv:1208.4185 [hep-lat].
- [108] M. Engelhardt, (2012), arXiv:1210.0025 [hep-lat].
- [109] W. Freeman and D. Toussaint (MILC), (2012), arXiv:1204.3866 [hep-lat].
- [110] P. E. Shanahan, A. W. Thomas, and R. D. Young, Phys. Rev. **D87**, 074503 (2013), arXiv:1205.5365 [nucl-th].
- [111] P. Junnarkar and A. Walker-Loud, (2013), arXiv:1301.1114 [hep-lat].
- [112] J. Ellis, K. A. Olive, and P. Sandick, New J.Phys. **11**, 105015 (2009), arXiv:0905.0107 [hep-ph].
- [113] M. Gong *et al.* (χ QCD Collaboration), “Strangeness and charm content of nucleon from overlap fermions on 2+1-flavor domain-wall fermion configurations,” (2013), arXiv:1304.1194 [hep-ph].
- [114] A. Bottino, F. Donato, N. Fornengo, and S. Scopel, Astropart. Phys. **13**, 215 (2000), arXiv:hep-ph/9909228 [hep-ph].
- [115] J. R. Ellis, K. A. Olive, and C. Savage, Phys. Rev. **D77**, 065026 (2008), arXiv:0801.3656 [hep-ph].
- [116] R. J. Hill and M. P. Solon, Phys. Lett. **B707**, 539 (2012), arXiv:1111.0016 [hep-ph].
- [117] H.-W. Lin, (2011), arXiv:1109.2542 [hep-lat].
- [118] C. Llewellyn Smith, Phys.Rept. **3**, 261 (1972).
- [119] J. Arrington, C. Roberts, and J. Zanotti, J.Phys. **G34**, S23 (2007), arXiv:nucl-th/0611050 [nucl-th].
- [120] A. Aguilar-Arevalo *et al.* (MiniBooNE Collaboration), Phys.Rev. **D81**, 092005 (2010), arXiv:1002.2680 [hep-ex].

- [121] B. Bhattacharya, R. J. Hill, and G. Paz, Phys.Rev. **D84**, 073006 (2011), arXiv:1108.0423 [hep-ph].
- [122] M. Day and K. S. McFarland, Phys.Rev. **D86**, 053003 (2012), arXiv:1206.6745 [hep-ph].
- [123] P. Coloma, P. Huber, J. Kopp, and W. Winter, Phys.Rev. **D87**, 033004 (2013), arXiv:1209.5973 [hep-ph].
- [124] R. J. Hill and G. Paz, Phys.Rev. **D82**, 113005 (2010), arXiv:1008.4619 [hep-ph].
- [125] J. A. Bailey *et al.* (Fermilab Lattice and MILC), Phys. Rev. **D79**, 054507 (2009), arXiv:0811.3640 [hep-lat].
- [126] A. A. Khan *et al.*, Phys. Rev. **D74**, 094508 (2006), arXiv:hep-lat/0603028.
- [127] T. Yamazaki *et al.*, Phys. Rev. **D79**, 114505 (2009), arXiv:0904.2039 [hep-lat].
- [128] J. D. Bratt *et al.* (LHP), Phys. Rev. **D82**, 094502 (2010), arXiv:1001.3620 [hep-lat].
- [129] C. Alexandrou *et al.* (ETM Collaboration), Phys.Rev. **D83**, 045010 (2011), arXiv:1012.0857 [hep-lat].
- [130] P. Hagler, Phys.Rept. **490**, 49 (2010), arXiv:0912.5483 [hep-lat].
- [131] S. Capitani, M. Della Morte, G. von Hippel, B. Jager, A. Juttner, *et al.*, Phys.Rev. **D86**, 074502 (2012), arXiv:1205.0180 [hep-lat].
- [132] R. Horsley, Y. Nakamura, A. Nobile, P. Rakow, G. Schierholz, *et al.*, (2013), arXiv:1302.2233 [hep-lat].
- [133] Y. Aoki, E. Shintani, and A. Soni, (2013), arXiv:1304.7424 [hep-lat].
- [134] R. N. Mohapatra and R. E. Marshak, Phys. Rev. Lett. **44**, 1316 (1980).
- [135] K. Genezer, *Proceedings of Workshop on B – L Violation* (2012) web page.
- [136] M. Baldo-Ceolin *et al.*, Z. Phys. **C63**, 409 (1994).
- [137] M. I. Buchoff, C. Schroeder, and J. Wasem, (2012), arXiv:1207.3832 [hep-lat].
- [138] M. Pospelov and A. Ritz, Ann. Phys. **318**, 119 (2005), arXiv:hep-ph/0504231 [hep-ph].
- [139] J. Engel, M. J. Ramsey-Musolf, and U. van Kolck, Prog.Part.Nucl.Phys. **71**, 21 (2013), arXiv:1303.2371 [nucl-th].
- [140] E. Shintani, S. Aoki, and Y. Kuramashi, Phys. Rev. **D78**, 014503 (2008), arXiv:0803.0797 [hep-lat].
- [141] T. Bhattacharya, V. Cirigliano, and R. Gupta, PoS **LATTICE2012**, 179 (2012), arXiv:1212.4918 [hep-lat].
- [142] R. Babich *et al.*, Phys. Rev. **D85**, 054510 (2012), arXiv:1012.0562 [hep-lat].
- [143] G. S. Bali *et al.* (QCDSF), Phys. Rev. Lett. **108**, 222001 (2012), arXiv:1112.3354 [hep-lat].
- [144] T. Bhattacharya *et al.*, Phys. Rev. **85**, 054512 (2012), arXiv:1110.6448 [hep-ph].
- [145] J. R. Green *et al.*, (2012), arXiv:1206.4527 [hep-lat].
- [146] H.-W. Lin, (2011), arXiv:1112.2435 [hep-lat].
- [147] A. Denner, S. Heinemeyer, I. Puljak, D. Rebuszi, and M. Spira, Eur.Phys.J. **C71**, 1753 (2011), arXiv:1107.5909 [hep-ph].
- [148] I. Allison *et al.* (HPQCD Collaboration), Phys.Rev. **D78**, 054513 (2008), arXiv:0805.2999 [hep-lat].
- [149] J. Beringer *et al.* (Particle Data Group), Phys. Rev. **D86**, 010001 (2012).
- [150] B. Blossier *et al.* (ETM), Phys. Rev. Lett. **108**, 262002 (2012), arXiv:1201.5770 [hep-ph].
- [151] P. M. Vranas, Phys. Rev. **D74**, 034512 (2006), arXiv:hep-lat/0606014 [hep-lat].
- [152] A. Stathopoulos and K. Orginos, SIAM J. Sci. Comput. **32**, 439 (2010), arXiv:0707.0131 [hep-lat].
- [153] G. P. Lepage, Phys. Rev. **D59**, 074502 (1999), arXiv:hep-lat/9809157 [hep-lat].
- [154] K. Orginos, D. Toussaint, and R. L. Sugar (MILC), Phys. Rev. **D60**, 054503 (1999),

- arXiv:hep-lat/9903032 [hep-lat].
- [155] A. X. El-Khadra, A. S. Kronfeld, and P. B. Mackenzie, *Phys. Rev.* **D55**, 3933 (1997), arXiv:hep-lat/9604004 [hep-lat].
 - [156] B. A. Thacker and G. P. Lepage, *Phys. Rev.* **D43**, 196 (1991).
 - [157] A. Bazavov *et al.* (MILC), PoS **LATTICE2010**, 074 (2010), arXiv:1012.0868 [hep-lat].
 - [158] P. A. Boyle *et al.* (RBC and UKQCD), *Eur. Phys. J.* **C69**, 159 (2010), arXiv:1004.0886 [hep-lat].
 - [159] V. Lubicz, F. Mescia, S. Simula, and C. Tarantino (ETM), *Phys. Rev.* **D80**, 111502 (2009), arXiv:0906.4728 [hep-lat].
 - [160] H. Na, C. T. H. Davies, E. Follana, G. P. Lepage, and J. Shigemitsu (HPQCD), *Phys. Rev.* **D86**, 054510 (2012), arXiv:1206.4936 [hep-lat].
 - [161] H. Na *et al.* (HPQCD), (2012), arXiv:1212.0586 [hep-lat].
 - [162] A. Bazavov *et al.* (Fermilab Lattice and MILC), (2012), arXiv:1210.8431 [hep-lat].
 - [163] H. Na, C. T. H. Davies, E. Follana, G. P. Lepage, and J. Shigemitsu (HPQCD), *Phys. Rev.* **D82**, 114506 (2010), arXiv:1008.4562 [hep-lat].
 - [164] H. Na *et al.* (HPQCD), *Phys. Rev.* **D84**, 114505 (2011), arXiv:1109.1501 [hep-lat].
 - [165] J. A. Bailey *et al.* (Fermilab Lattice and MILC), (2012), arXiv:1211.4964 [hep-lat].
 - [166] Y. Amhis *et al.* (Heavy Flavor Averaging Group), (2012), arXiv:1207.1158 [hep-ex].
 - [167] S.-W. Qiu *et al.* (Fermilab Lattice and MILC), PoS **LATTICE2011**, 289 (2011), arXiv:1111.0677 [hep-lat].
 - [168] J. A. Bailey *et al.* (Fermilab Lattice and MILC), *Phys. Rev.* **D85**, 114502 (2012), arXiv:1202.6346 [hep-lat].
 - [169] E. Dalgic *et al.* (HPQCD), *Phys. Rev.* **D73**, 074502 (2006), arXiv:hep-lat/0601021 [hep-lat].
 - [170] F. Bahr *et al.*, (2012), arXiv:1211.6327 [hep-lat].
 - [171] C. M. Bouchard, G. P. Lepage, C. J. Monahan, H. Na, and J. Shigemitsu, PoS **LATTICE2012**, 118 (2012), arXiv:1210.6992 [hep-lat].
 - [172] H. Na *et al.*, *Phys. Rev.* **D86**, 034506 (2012), arXiv:1202.4914 [hep-lat].
 - [173] A. Bazavov *et al.* (Fermilab Lattice and MILC), *Phys. Rev.* **D85**, 114506 (2012), arXiv:1112.3051 [hep-lat].
 - [174] N. Carrasco *et al.*, PoS **ICHEP2012**, 428 (2012), arXiv:1212.0301 [hep-ph].
 - [175] F. Bernardoni *et al.*, (2012), arXiv:1210.7932 [hep-lat].
 - [176] E. Gámiz, C. T. H. Davies, G. P. Lepage, J. Shigemitsu, and M. Wingate (HPQCD), *Phys. Rev.* **D80**, 014503 (2009), arXiv:0902.1815 [hep-lat].
 - [177] A. Bazavov *et al.* (Fermilab Lattice and MILC), *Phys. Rev.* **D86**, 034503 (2012), arXiv:1205.7013 [hep-lat].
 - [178] S. Dürr *et al.*, *Phys. Lett.* **B705**, 477 (2011), arXiv:1106.3230 [hep-lat].
 - [179] D. J. Antonio *et al.* (RBC and UKQCD), *Phys. Rev. Lett.* **100**, 032001 (2008), arXiv:hep-ph/0702042 [HEP-PH].
 - [180] R. Arthur *et al.* (RBC and UKQCD), (2012), arXiv:1208.4412 [hep-lat].
 - [181] C. Aubin, J. Laiho, and R. S. Van de Water, *Phys. Rev.* **D81**, 014507 (2010), arXiv:0905.3947 [hep-lat].
 - [182] T. Bae *et al.*, *Phys. Rev. Lett.* **109**, 041601 (2012), arXiv:1111.5698 [hep-lat].
 - [183] C. Kelly (RBC and UKQCD), PoS **LAT2012** (2012).
 - [184] G. Martinelli, C. Pittori, C. T. Sachrajda, M. Testa, and A. Vladikas, *Nucl. Phys.* **B445**, 81 (1995), hep-lat/9411010.
 - [185] V. Cirigliano, G. Ecker, H. Neufeld, A. Pich, and J. Portoles, *Rev.Mod.Phys.* **84**, 399 (2012),

- arXiv:1107.6001 [hep-ph].
- [186] C. Sachrajda (Brookhaven National Lab, May, 2012).